DGE/1523-2
Distribution Category UC-66d

HEAT TRANSFER CHARACTERISTICS OF A SURFACE TYPE DIRECT CONTACT BOILER

Robert S. Deeds
Harold R. Jacobs
Robert F. Boehm

MECHANICAL ENGINEERING
UNIVERSITY OF UTAH
SALT LAKE CITY, UTAH 84112
Date Published--March 1976

PREPARED FOR THE
ENERGY RESEARCH AND DEVELOPMENT ADMINISTRATION
DIVISION OF GEOTHERMAL ENERGY
UNDER CONTRACT E(10-1)1523

DISCLAIMER

ABSTRACT

Use of a direct contact heat exchanger in a secondary power cycle has recently been proposed as a means of utilizing geothermal energy in brine form. The use of a direct contact heat exchanger in this type of application would be very desirable due to the high overall heat transfer coefficients obtainable and the elimination of the effect of scaling upon heat transfer.

In this study, two direct contact heat exchangers were constructed and test results were obtained using water and refrigerant 113 as the working fluids. The heat exchangers were operated in a three-phase mode; the water remained liquid throughout the vessel and the liquid refrigerant 113 underwent vaporization following direct injection into the water.

The effect of important operational parameters - operating heights, refrigerant 113 injection techniques, mass flow ratios, and temperatures - was studied to determine generalized trends important in the design and operation of a prototype three-phase direct contact heat exchanger.

The primary system used in this study performed well overall. The initial favorable results of this study warrant further investigation of direct contact heat exchange as a means of utilizing geothermal energy.

ACKNOWLEDGEMENTS

This work resulted from the Master of Science in Mechanical Engineering Thesis by the first author. Appreciation is expressed to the Raft River Geothermal Project of ERDA for providing funding for the study, and to DuPont for donations of Freon 113.

TABLE OF CONTENTS

LIST OF FIGURES

Figure

LIST OF TABLES

I. INTRODUCTION

Direct contact between droplets of a volatile fluid dispersed within an immiscible liquid medium provides an excellent potential for heat exchange. Heat transfer coefficients for direct contact heat exchange have been reported by Sideman and Taitel [1] as being one or two orders of magnitude greater than the heat transfer coefficients for processes utilizing metallic heat transfer surfaces. Other advantages include: a) larger, more effective heat transfer areas; b) elimination of the scaling problem on heat transfer surfaces; c) less severe corrosion problems; d) relatively simple equipment design. These advantages make direct contact heat exchange applicable to a wide variety of industrial applications. The disadvantages of this type of heat exchanger are basically centered around the potential loss of working fluid. However, selection of proper fluids and present separation techniques can largely reduce this problem.

Direct contact heat exchange has been the subject of numerous articles; the majority of which have dealt with two phase systems, i.e., systems in which heat is transferred from one fluid in the liquid phase to a second fluid also in the liquid phase. Recently, however, three phase systems have been investigated as possible desalinization techniques for sea water [2,3,4]. In this technique a secondary fluid is boiled off in the sea water forming small ice crystals. These

crystals can then be separated and melted to yield fresh water. A second method is to boil the sea water using direct contact heat transfer with a heavy organic liquid heated to a temperature above the saturation temperature of the sea water. The vapor that is evolved can then be condensed to produce the fresh water. A preliminary economic assessment of the latter method has been shown to compare favorably with other desalinization processes [5].

Three phase systems have also been proposed as a means of extracting heat from geothermal brines [6]. The hot geothermal brine is used to boil a secondary fluid and the resulting vapor is used in a binary power cycle.

Single drop studies have been carried out by several authors [1,7,8] for volume type three phase direct contact heat exchangers. The term "volume type" here refers to heat exchangers in which the volatile liquid is injected directly into the continuous liquid medium. Sideman and Taitel obtained heat transfer coefficients of about 350 $W/(m^2°C)$ for nonevaporating droplets, while, for droplets of the same initial drop diameter (3.5 mm) that completely evaporated, coefficients on the order of 23,000 $W/(m^2°C)$ were obtained. Similar results were obtained by Wilke [5] using a heavy organic liquid as the continuous phase and water as the volatile phase. These papers indicate the large advantage of utilizing heat transfer processes with change of phase.

Simpson et. al. [9,10] also studied the evaporation of a single drop immersed in a continuous immiscible phase and proposed

a new mathematical model. More recently, Jacobs and Thomas [11] developed an integral analysis for the evaporation of a single spherical drop in an immiscible medium.

Very little information is available concerning single drop studies for surface boiling three phase direct contact heat exchangers. The term "surface boiling" here refers to heat exchange in which the volatile liquid is sprayed onto the surface of the continuous liquid medium. A paper by Waldram et. al. [12] discussed a system where small droplets of various organic liquids, boiling somewhat above room temperature, were allowed to fall on a shallow layer of hot silicone oil. A discussion of the various modes of heat transfer and the physical conditions necessary to produce these modes is presented; however, nothing is mentioned as to the heat transfer rates attained.

Single drop studies and the associated theory on the heat transfer mechanism involved may not be directly extended to situations where large numbers of droplets are present in a dispersed phase due to arbitrary nucleation times and droplet coalescence. Sideman and Gat [13] studied the problem of a multiple drop three phase direct contact heat transfer using a volume type boiler, with the intent of experimentally determining the transfer characteristics of a small scale laboratory model under various operating conditions using pentane and water. In this study the volatile fluid (pentane) had a lower density than the continuous phase fluid (water). Thus, evaporation occurred as the volatile droplets rose through the

continuous phase fluid. The results of this study were presented using a volumetric heat transfer coefficient defined as:

$$U_v = Q/V\Delta T \qquad (1)$$

where temperature driving force ΔT was approximated by the logarithmic mean temperature difference assuming counter-current flow. Values of this coefficient were reported as being as high as $2.3 \times 10^5 W/(m^3 {}^\circ C)$.

Somers et. al. [14,15] studied the evaporation of sea water sprayed onto a layer of hot mineral oil, the mineral oil being less dense than the water. It was observed that the water drops partly flashed at the surface of the oil while the remaining portions immediately sank into the oil phase. Although the heat transfer appeared most promising, a foam formation occurred due to extensive boiling below the surface of the mineral oil. This may well have been due to the emulsion characteristics of the water-mineral oil system.

An experimental study of the transient boiling rates of various cryogens on a water surface has been reported by Drake et. al. [16,17]. In these experiments, a layer of the cryogen was introduced onto the surface of a layer of water. The cryogen was allowed to boil off, and the evaporation rates were measured. Since the density of the cryogens was less than the density of the water, all of the boiling took place at the water-cryogen interface. In

addition, since the cryogens boil at temperatures below the freezing point of water, it was observed that ice formed at the interface of the two fluids and extended into the water. The heat transfer therefore took place on a water-ice surface or a solid ice or hydrate crust formed very early in the run. This type of system would best be described as a four phase system in contrast to the three phase systems previously discussed.

It is the purpose of this paper to experimentally evaluate a surface boiling multiple drop three phase direct contact heat exchanger, in contrast to the volume boiling exchanger discussed by Sideman and Gat [13]. The surface boiling exchanger has the advantage that the injection nozzle used for the volatile fluid need not come in contact with the continuous phase fluid. This is especially advantageous in cases where the continuous phase fluid is corrosive and/or presents possible scaling problems. It is also much easier to atomize the volatile fluid by spraying it into a vapor region than by injecting it into a liquid region. Better atomization results in larger heat transfer surfaces, and thus more effective heat transfer. Atomizing or spray nozzles do, however, present the problem of slightly higher pressure drops than liquid jet nozzles as a trade off to the larger heat transfer areas.

Experiments were conducted on a small scale laboratory model using Refrigerant 113 as the volatile fluid and water as the continuous phase fluid. In these experiments, R-113 was sprayed onto the surface of a two inch layer of heated water using a low capacity

pressure nozzle producing a finely atomized hollow cone spray pattern. The R-113 was boiled out of the water and the vapor was collected, condensed, and recycled. Pertinent temperatures, pressures and flow rates were recorded and evaluated and are presented in the form of performance curves with particular interest placed on the effects of flow rates and temperature variations on the overall heat flow rate. Results are also presented which define operating conditions necessary to produce complete boiling of the R-113 and the conditions are shown at which incomplete boiling begins to occur. A nondimensional equation is derived describing the performance of the test apparatus for the range of operating conditions investigated.

II. EXPERIMENTAL APPARATUS

A. System

A schematic of the system used to supply the test vessel is shown in Figure 1. This system can be divided into two subsystems; one supplying water to the test vessel and the other supplying the R-113.

1. Water Side

The water was heated in a stainless steel kettle. Steam, supplied by a large boiler in the building, was run through a jacket in the bottom portion of the kettle to supply the heat. A 1.27 cm needle valve located on the steam inlet line provided temperature control within the kettle. Supply tank temperature was measured using a chromel-alumel thermocouple with an accuracy of $\pm$ 1.0 °C. A drain line was constructed at the bottom of the kettle and a fresh water fill line was supplied at the top to allow for frequent changes of water, insuring that clean water was used in all of the tests.

Hot water was pumped out of the kettle using a centrifugal pump. A bypass line was provided after the pump to reduce the loading on the pump and to allow for more stable water flow control.

Water flow rates were measured using one of two F. & P. Rotameters. The first rotameter covered a range of 0 to 56 liters/hr

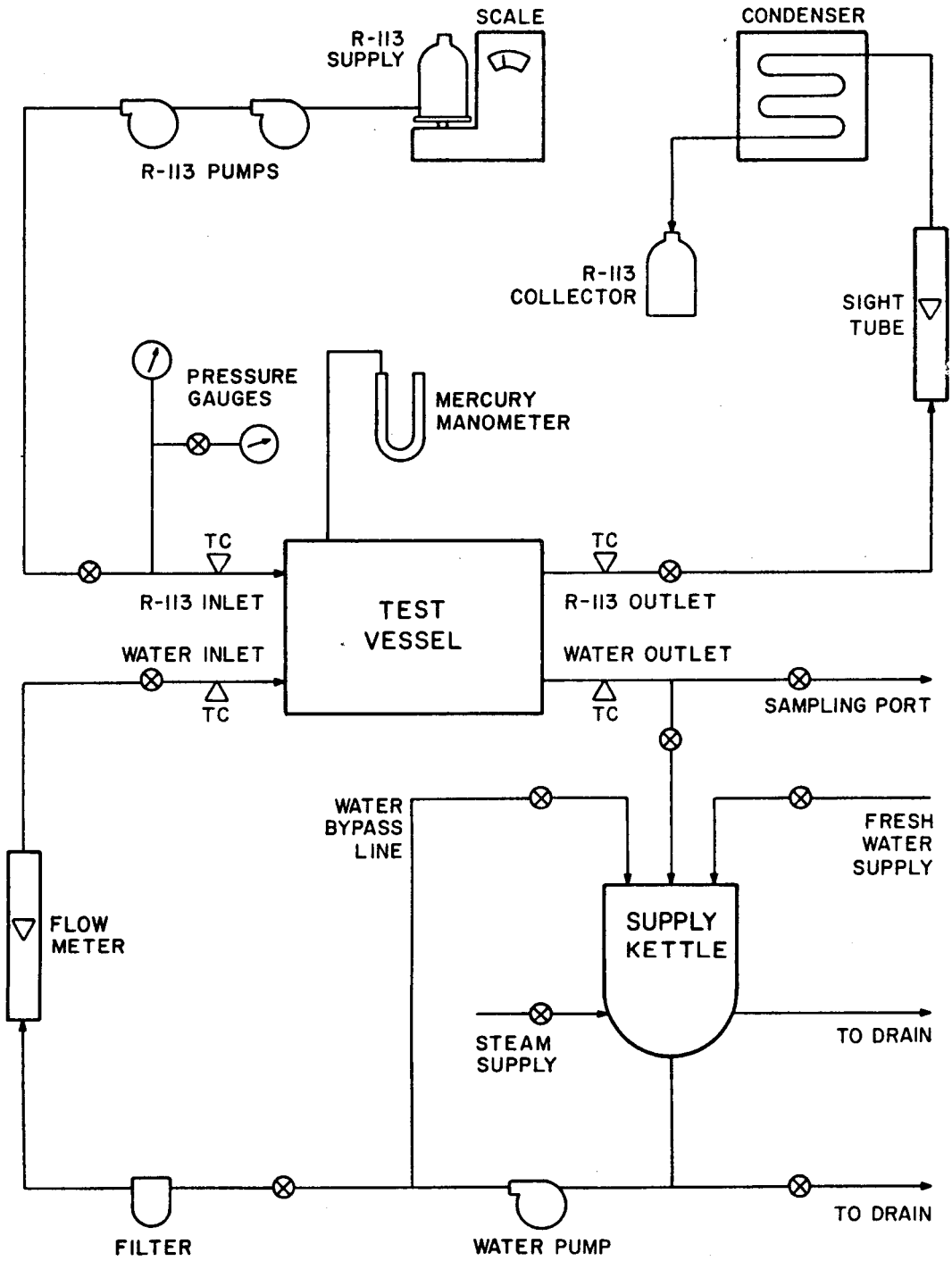

Figure 1. Schematic of System

with a calibrated accuracy of ± 1.0% of full scale. The second flow meter had a range of 0 to 114 liters/hr with a calibrated accuracy of ± 1.0% of full scale. Due to slight fluctuations in flow rates, accuracy during the experiments was reduced to ± 1.5 liters/hr for both flow meters. A gasoline filter was placed before the flow meter to prevent distortion in the readings caused by clogging or scaling within the flow meter. A 1.27 cm needle valve was placed between the filter and the flow meter to provide flow control.

Water leaving the flow meter proceeded to the test vessel at which point the temperature at the vessel inlet was measured. The temperature of the water leaving the vessel was measured directly after the vessel. Both inlet and outlet temperatures were measured using chromel-alumel thermocouples calibrated to ± 0.1 °C. Water leaving the vessel was routed back to the heating kettle to be recycled. A sample port was placed in the water return line to determine if R-113 was being carried out with the water.

2. R-113 Side

R-113 was supplied to the test vessel from a weighing tank located on a set of scales. From the weighing tank, the R-113 was pumped to the test vessel using two centrifugal pumps in series, providing a line pressure of up to 138 kPa. Line pressure between the pumps and the vessel was measured using one of two pressure gauges, a 0 to 414 kPa gauge or a 0 to 103 kPa gauge. Most of the test runs were conducted within ranges where the smaller gauge was used;

however, some of the higher flow rates required use of the larger gauge. The 0 to 103 kPa gauge was calibrated using a mercury manometer to $\pm$ 3.0% of full scale. The 0 to 414 kPa gauge was calibrated using a mercury manometer to $\pm$ 3.0% of full scale for pressures up to 207 kPa. R-113 flow was regulated using a 0.635 cm needle valve located after the pumps and before the pressure gauges.

After the pressure gauges, the R-113 was directed to the test vessel. At the test vessel, the temperatures of the R-113 entering the vessel and the vapor leaving the vessel were measured using chromel-alumel thermocouples calibrated to $\pm$ 0.1 °C.

The vapor then flowed to a gas phase flow meter. When R-113 flow was initiated, the temperature of the walls of this flow meter were lower than the saturation temperatures of both the R-113 vapors and the water vapors leaving the vessel. This caused portions of these vapors to condense and build up within the flow meter. When the system had run long enough for it to come to steady state, the R-113 that had collected in this flow meterbegan to boil off; however, the temperature within the flow meter was still insufficient to evaporate the water. Thus there was always a finite amount of liquid in this flowmeter which prevented its use as a flow measuring device, and therefore, it was used merely as a sight tube.

From the flow meter, the vapor was taken to a finned tube heat exchanger to be condensed. The condensate was collected in a second storage tank.

B. Vessel

A schematic of the test vessel is shown in Figure 2 with a photograph of the vessel shown in Figure 3. It consisted of 1.6 cm mild steel on four sides, with 0.48 cm tempered glass on the front and back. The top was removable to allow for modifications inside the vessel. A stainless steel tray was located 7.6 cm above the bottom of the vessel. This tray was used to provide a constant depth of water onto which the R-113 was sprayed. A drawing of the tray is shown in Figure 4. It was constructed having three sides 7.62 cm high, with the remaining side 5.08 cm high. Referring to Figure 4, water entered the tray along Side B, flowed across the tray to Side A, and there was spilled over into the bottom of the vessel, thus providing a constant 5.08 cm water depth.

Looking now at Figure 2, water entered the vessel at point 1 through 1.27 cm copper tubing which continued along the bottom of the vessel until it turned up and into the tray at point 2. It then flowed across the tray and was spilled over at point 3. After spilling over, it proceeded along the bottom of the vessel to a 1.27 cm copper tubing drain line at point 4.

The R-113 entered the vessel at point 5 through 0.32 cm polyflow tubing. 0.64 cm copper tubing carried the R-113 from the vessel wall to a nozzle centered over the tray (point 6) from which it was sprayed onto the surface of the water from a height of 12.7 cm. The R-113 vapor left the vessel through 1.27 cm copper tubing at point 7.

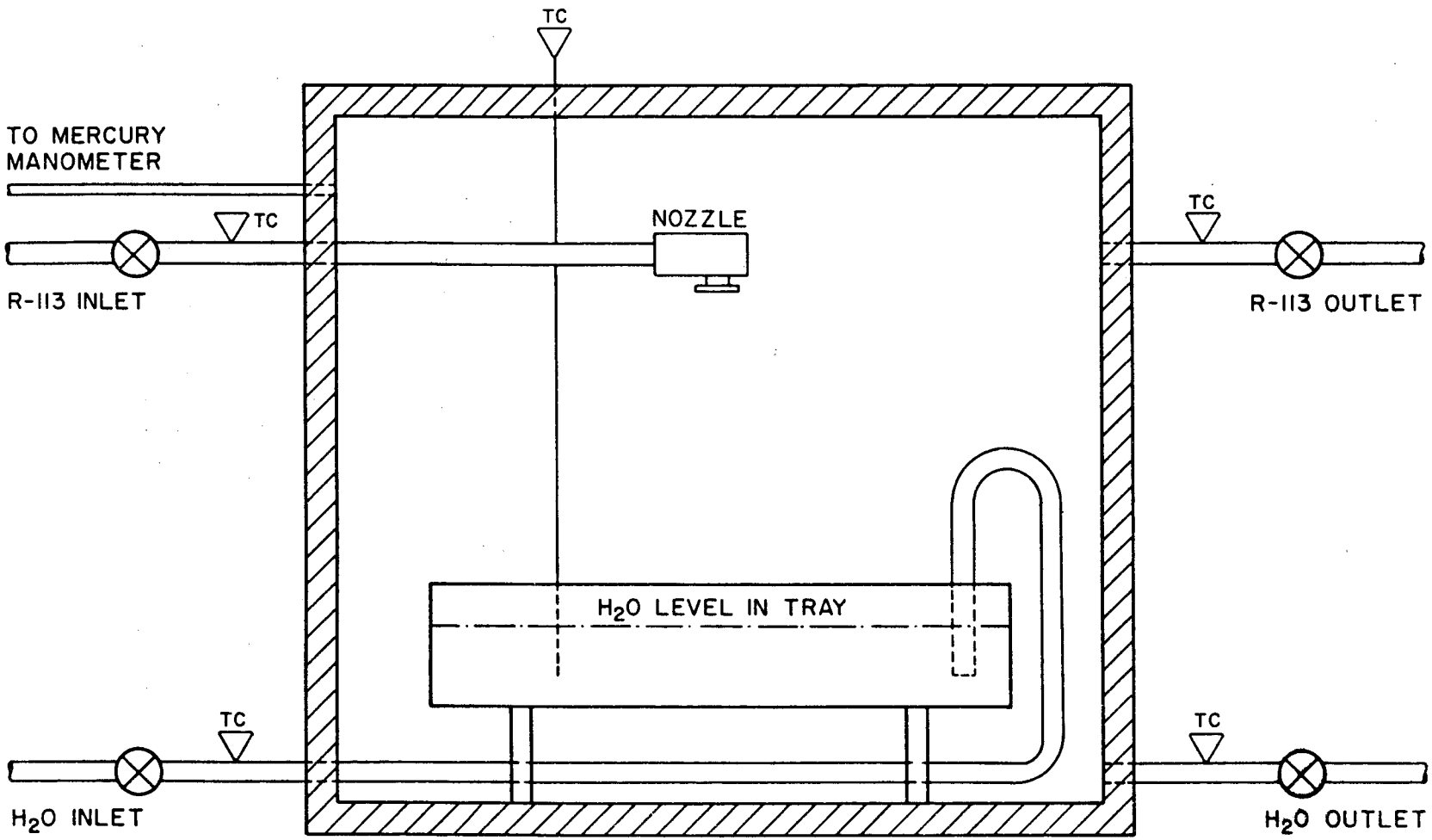

Figure 2. Schematic of Test Vessel

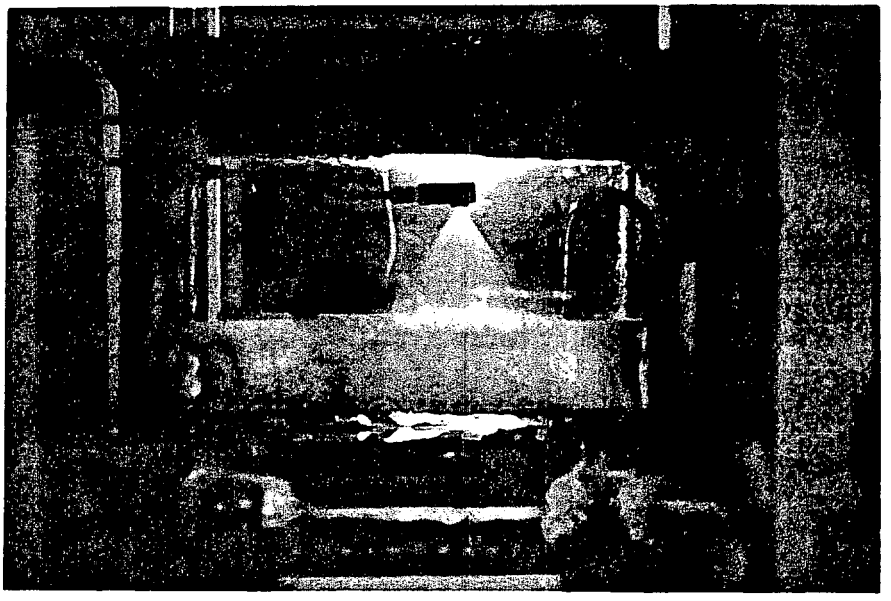

Figure 3. Test Vessel

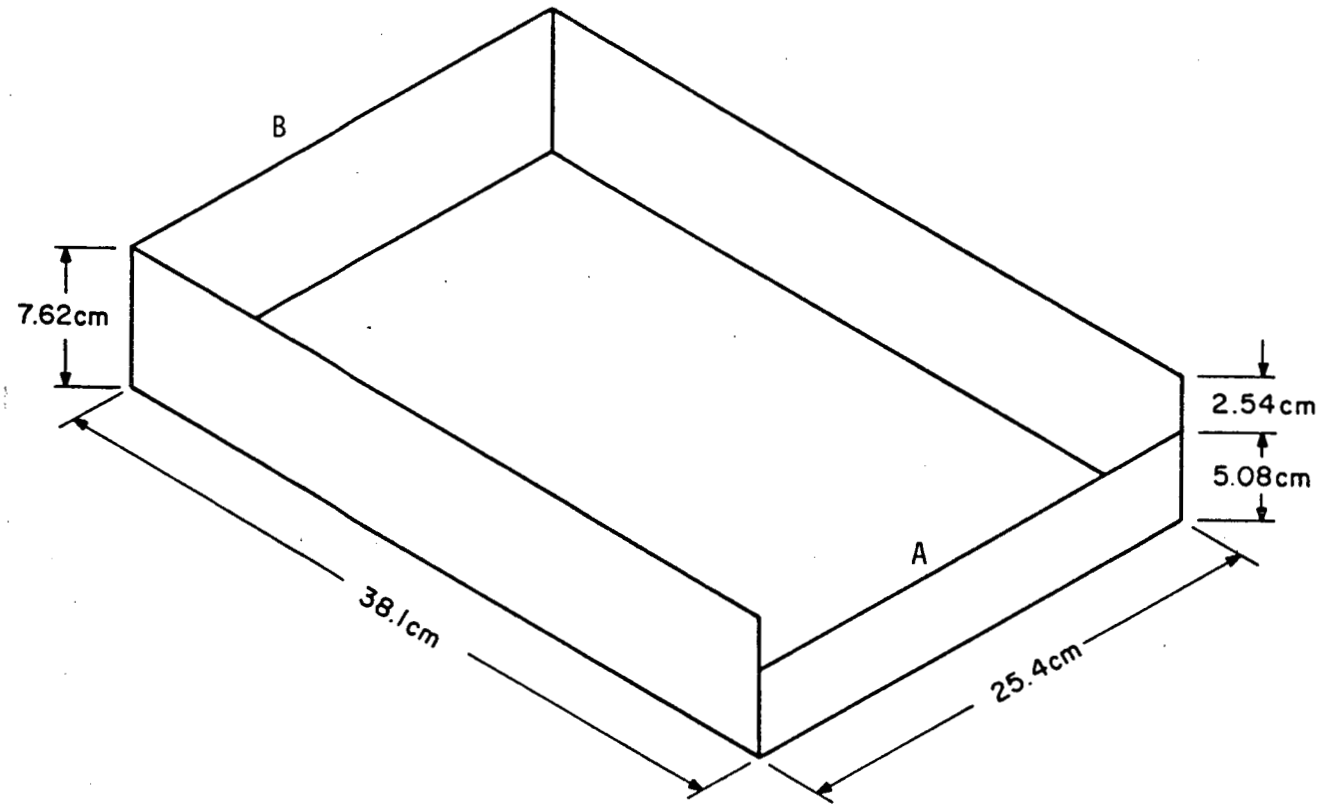

Figure 4. Tray Dimensions

Vessel pressure was measured by connecting a port in the side of the vessel (point 8) to a 122 cm mercury manometer. A chromel-alumel thermocouple calibrated to $\pm$ 0.1 °C was also provided to measure tray temperature. It entered the vessel through the top plate (point 9) with the bead being located half way between the front and back of the tray and 7.62 cm from the weir side of the tray. It was constructed to allow for variations in the height of the bead, thus providing a horizontal temperature profile in the tray.

The vessel was insulated on all sides using 7.72 cm polyurethane board to reduce heat losses to the environment. (A discussion of heat loss is given in Appendix I). Two small holes were cut in the insulation, one in the front and one in the back of the vessel, to allow for visual observation inside the vessel.

C. Nozzle

A drawing of the spray nozzle is shown in Figure 5 and the actual nozzle itself is shown in Figure 6. The nozzle is of two part construction consisting of a nozzle body and a spray insert. The nozzle body leads the R-113 tangentially into a swirl chamber and, after spinning in the swirl chamber, emerges through the orifice in the spray insert in the form of a hollow spinning column of liquid. As it reaches the outer edge of the orifice, droplets are flung off of the spinning column, thus producing a hollow cone spray pattern. This type of nozzle provides a spray with nominal droplet sizes of approximately 200 microns for design pressures of 138 kPa [18]. The

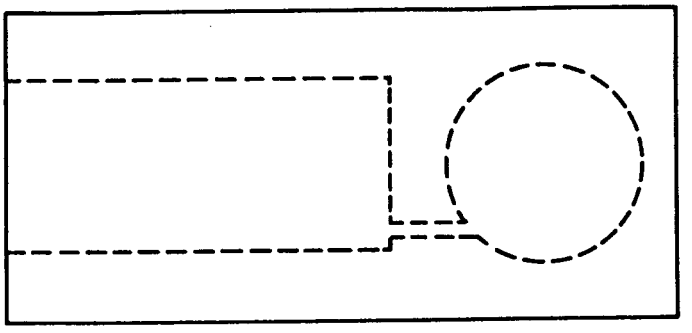

TOP VIEW

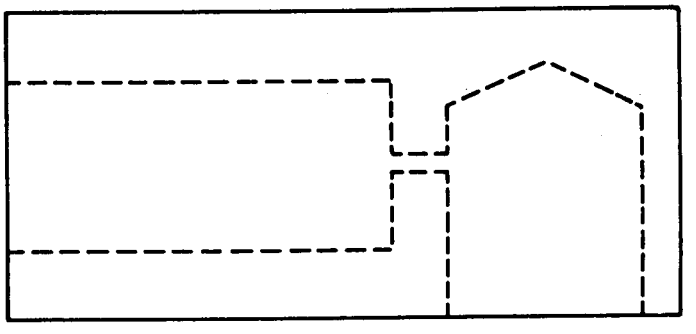

SIDE VIEW

NOZZLE BODY

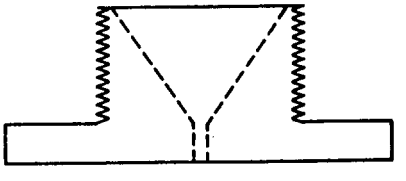

SPRAY INSERT

Figure 5. Schematic of Spray Nozzle

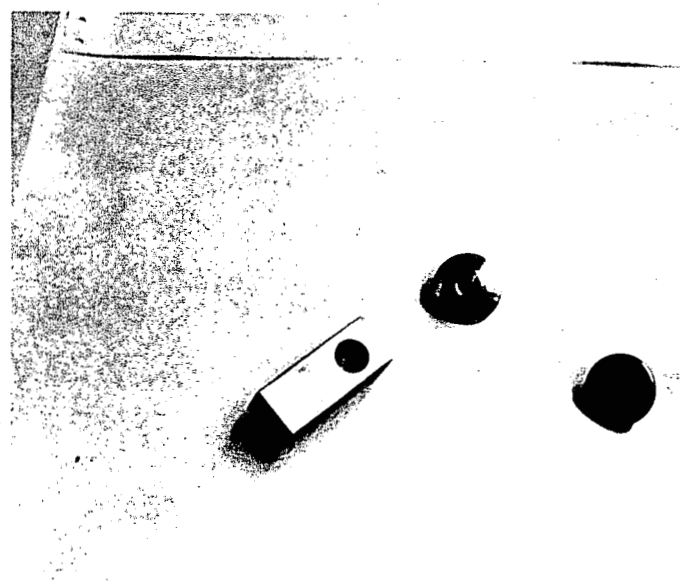

Figure 6. Spray Nozzle

spray strikes the surface of the water in the form of a ring with an inside diameter of 12.7 cm and an outside diameter of 17.8 cm. Full cone nozzles and square spray nozzles are commercially available and would possibly have been more effective for our purposes. However, these nozzles require larger pressure drops for the same flow rates and thus, due to our pumping restrictions, it was necessary to stay with the hollow cone pattern.

III. EXPERIMENTAL PROCEDURE

Data collection was essentially a straight forward and simple procedure. Water temperature in the kettle was set by adjusting steam flow to provide the desired water inlet temperature. Continuous monitoring of the thermocouple located in the kettle provided essentially constant vessel inlet temperature. Water flow was then set using the 1.27 cm needle valve located directly before the flow meter.

As has been previously mentioned, water entering the vessel was directed into the tray within the vessel from which it spilled over onto the bottom of the vessel and was drained. To prevent any of the R-113 vapor from being carried out through this drain line, it was necessary to have the water level in the bottom of the vessel completely cover the drain. All tests were therefore run with a water depth in the bottom of the vessel of approximately 7.62 cm. This level could be observed through the hole in the insulation and was controlled using the gate valve on the water exit line.

R-113 could now be supplied to the test vessel. R-113 flow rate was set using the line pressure gauges. Since the vessel was essentially at atmospheric pressure, these gauges read the approximate pressure drop across the nozzle. This pressure drop was calibrated against flow rate and gave readings of $\pm$ 1.9 liters/hr. Once set, the R-113 flow rate was measured to an even greater accuracy

using the scales on which the R-113 supply tank was located and a stop watch. The time it took for a given amount of R-113 (in a typical run this amounted to 1.8 kg) to leave the supply tank was measured yielding flow rates accurate to $\pm$ 0.2 liters/hr.

Temperatures were recorded using a two channel strip chart recorder and a digital voltmeter. During the course of a test, the voltmeter was used to monitor the temperature of the water in the supply kettle. By carefully controlling this temperature, the temperature at the vessel inlet was held constant throughout the experiment. The strip chart recorder was used to continually monitor the inlet and outlet water temperatures. Steady state operation was attained when the temperature of the water leaving the vessel became constant. Thus the strip chart recorder was used to determine whether or not steady state had occurred. Typical tests took approximately 45 minutes to stabilize. When steady state was reached, all thermocouple outputs were read using the digital voltmeter.

IV. DISCUSSION OF RESULTS

The results of this investigation consist essentially of performance data for the heat exchanger. The method used for data reduction is given in Appendix II. Appendix V contains all of the pertinent data for each of the figures discussed. This discussion will be presented in four sections: a) acceptable operating conditions; b) heat transfer characteristics; c) approach temperatures; and d) correlation equation.

A. Acceptable Operating Conditions

As mentioned in the Introduction, the major disadvantage of direct contact heat exchangers is the loss of working fluid. It is therefore necessary to determine at what point large scale carryover of R-113 occurs. Carryover is defined for the tray configuration used as the situation where a buildup of R-113 in the tray occurs. Large scale carryover results when incomplete boiling of the R-113 takes place. Liquid R-113 begins to build up in the heat exchanger tray until a point is reached at which this liquid R-113 is swept out of the heat exchanger with the water.

Figures 7, 8 and 9 show curves used to determine the point at which incomplete boiling occurs. The heat transferred to the R-113, represented by the square symbols, was calculated assuming

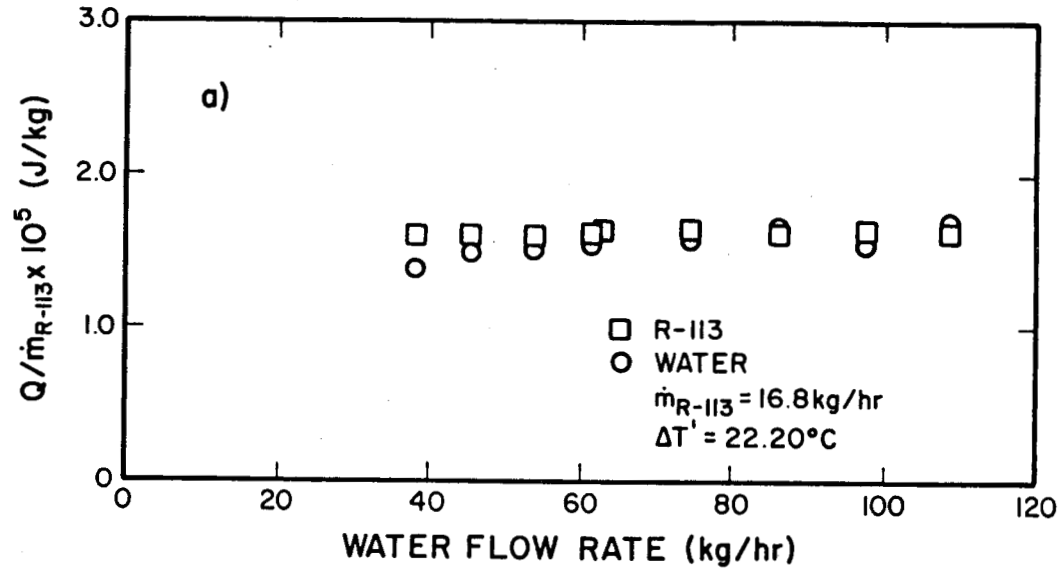

a.

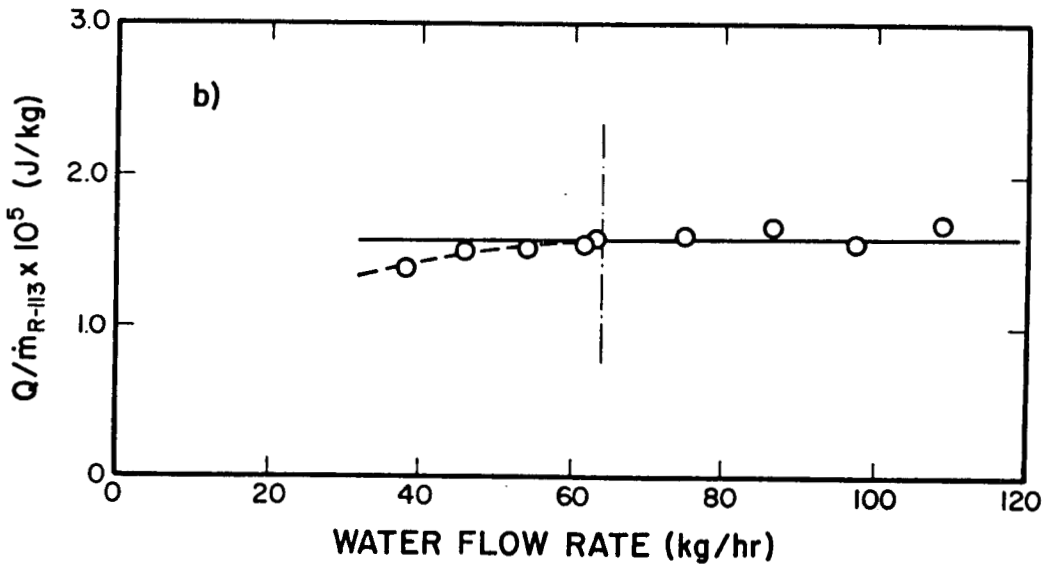

b.

Figure 7. Curve used for Determination of R-113 Buildup in Tray

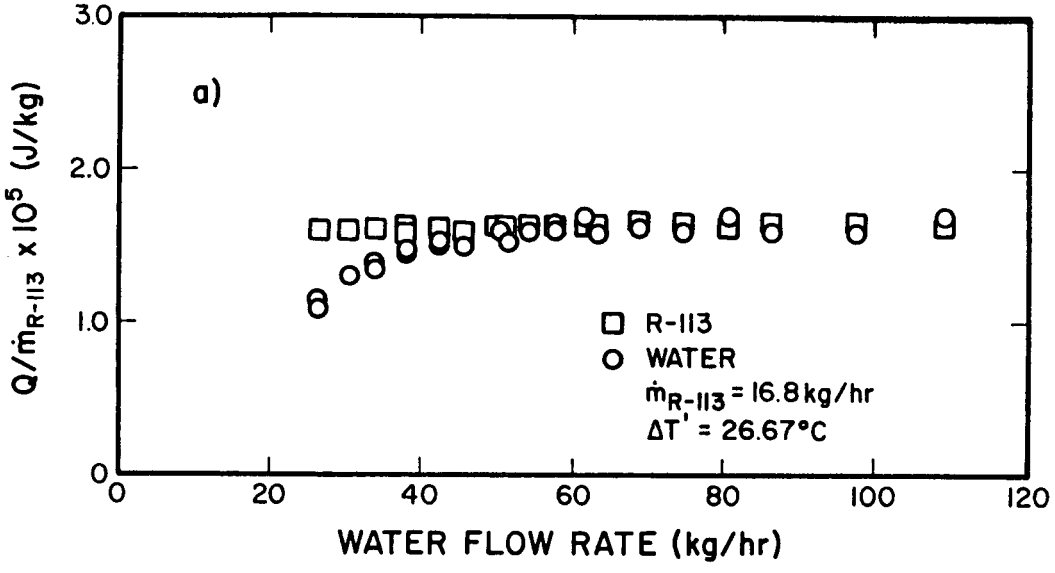

a.

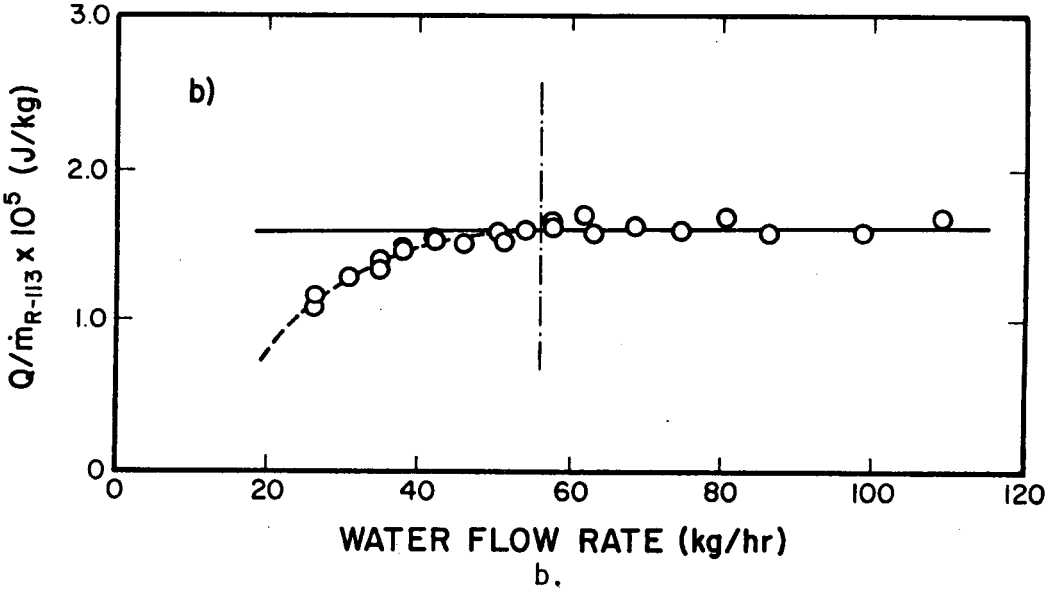

b.

Figure 8. Curve used for Determination of R-113 Buildup in Tray

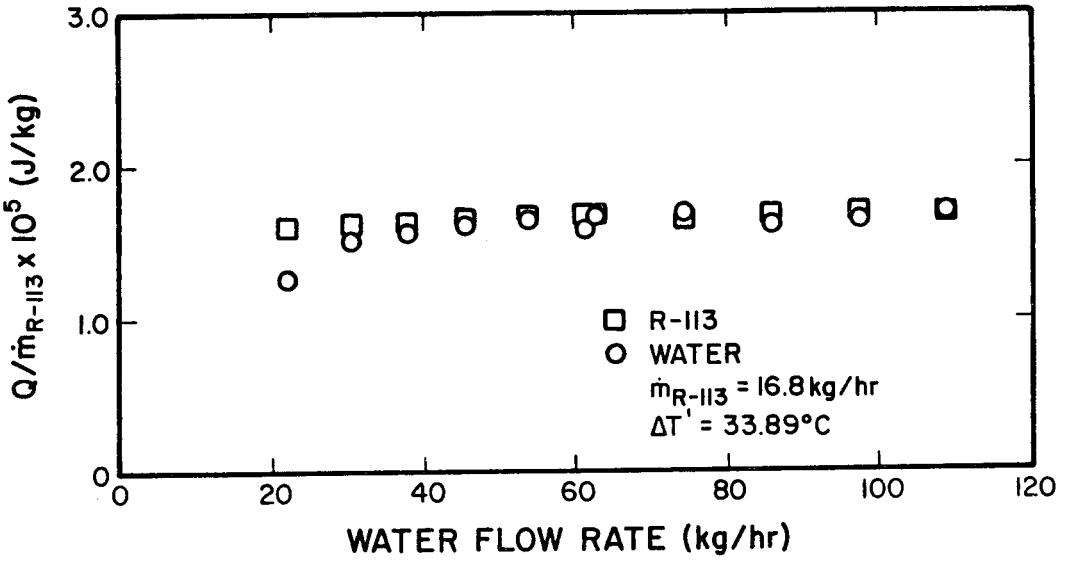

a.

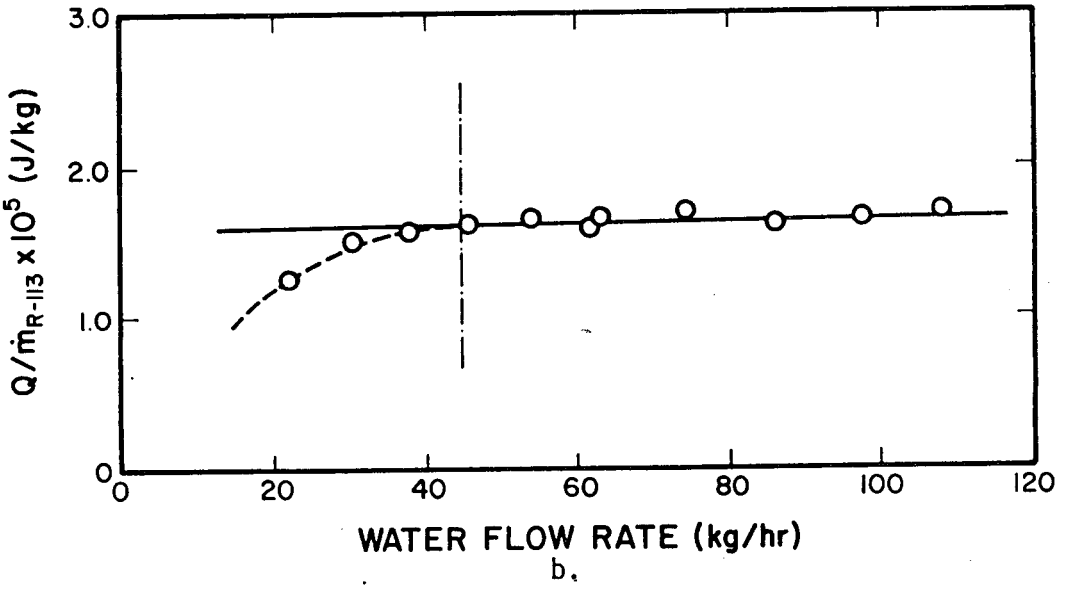

b.

Figure 9. Curve used for Determination of R-113 Buildup in Tray

that all of the R-113 was evaporated. The circular symbols represent the actual heat transferred as calculated from the water side. Both of the values of the transferred heat were divided by the mass flow rate of the R-113. The purpose of this procedure was to reduce any scatter in the data caused by slight fluctuations in the R-113 flow rate.

When complete boiling occurs, the two values of the transferred heat should coincide, as they do for the higher water flow rates. As the water flow rate decreases, however, the heat transferred from the water begins to drop below the R-113 curve. It is at this point that R-113 begins to build up. In Figures 7b, 8b and 9b, the R-113 data is fit to a least squares line to allow for a better means of determining the conditions when incomplete boiling occurs. Also shown (by the vertical dotted line) is the buildup point itself.

Figure 10 shows a compilation of the data from Figures 7, 8 and 9. Acceptable operating conditions are shown as a function of mass flow ratio and the temperature difference between the water inlet temperature and the R-113 saturation temperature ($\Delta T'$). For conditions above the curve, no buildup should be expected. For operating conditions below the curve, incomplete boiling of the R-113 will occur, and liquid R-113 is likely to be discharged through the water outlet line if the system is allowed to operate in these conditions.

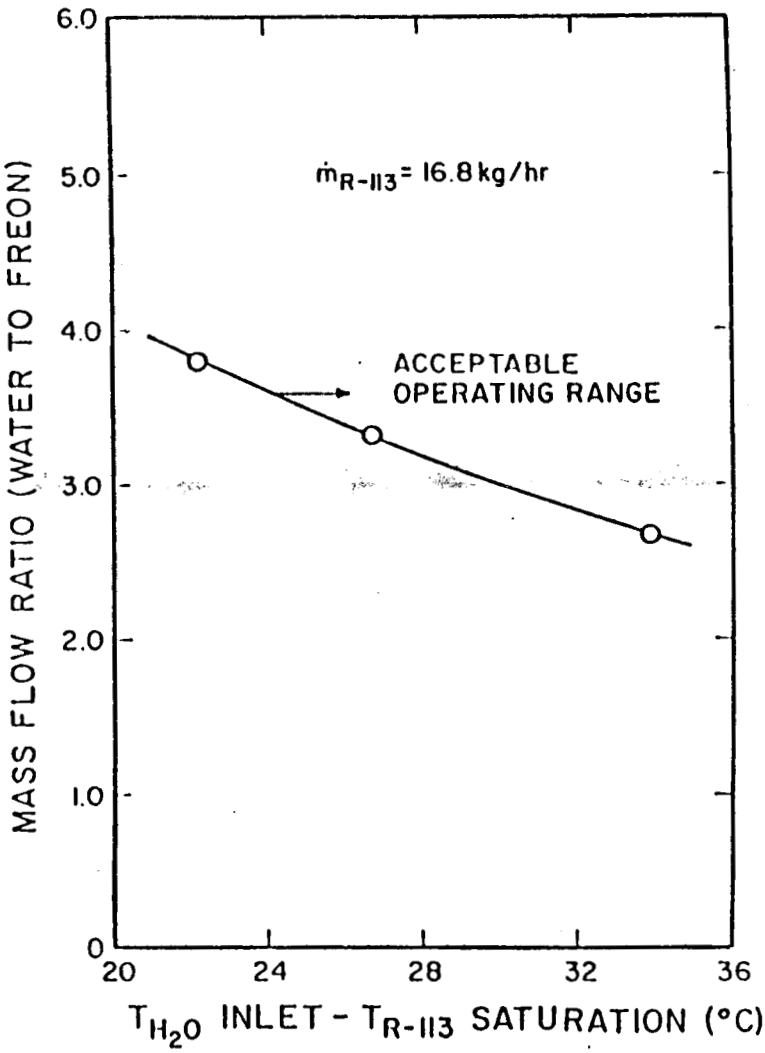

Figure 10. Acceptable Operating Range for R-113 Water System

B. Heat Transfer Characteristics

Within the acceptable operating conditions, it was necessary to evaluate the heat transfer process for various operating modes. To accomplish this, a UA factor was defined as the net heat transferred divided by the log mean temperature difference assuming counter-current flow. The area term was left in this heat transfer coefficient due to the difficulty of determining an appropriate area.

Figures 11, 12 and 13 illustrate the behavior of the UA factor as a function of $\Delta T'$, water flow rate, and R-113 flow rate. As can be seen from Figure 13, UA is strongly dependent on $\Delta T'$. The UA factor drops rapidly as $\Delta T'$ increases for the range of temperatures tested in this study. UA is effectively independent of water flow rate (Figure 12) as long as the water flow is sufficiently high to prevent buildup. Figure 13 shows the strong dependence of UA on R-113 flow rate. This figure shows a sharp rise in UA for increasing R-113 flow rates.

C. Approach Temperatures

Another important parameter involved in boiling heat transfer is the degree of superheat attained by the volatile fluid. For the optimum conditions, one would like to have the R-113 leave the vessel at its saturation temperature. This would mean that all of the heat was transferred in the highly efficient boiling mode rather than the less efficient heating of a vapor. However, some degree of superheat

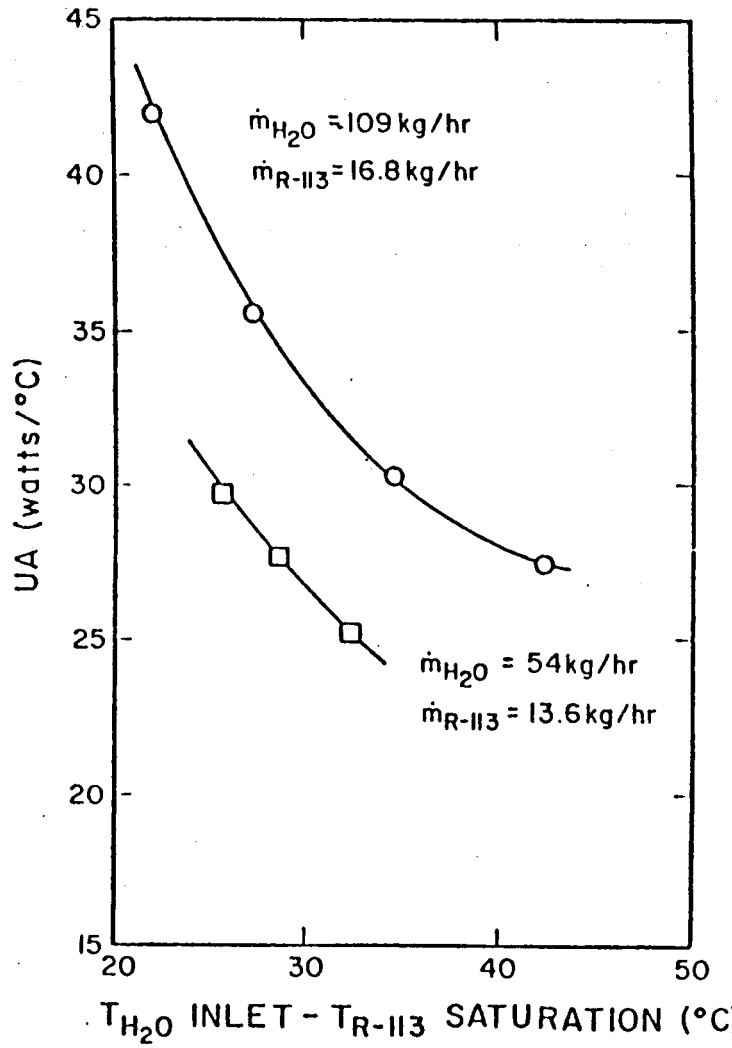

Figure 11. Effect of $\Delta T'$ on UA Factor

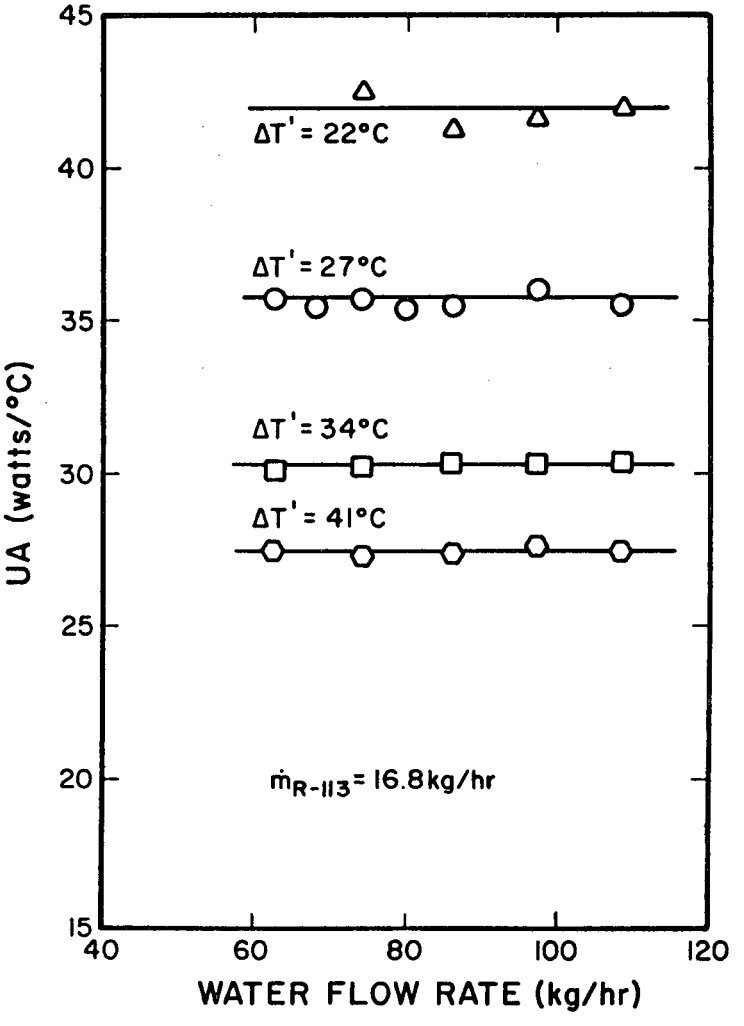

Figure 12. Effect of Water Flow Rate on UA Factor

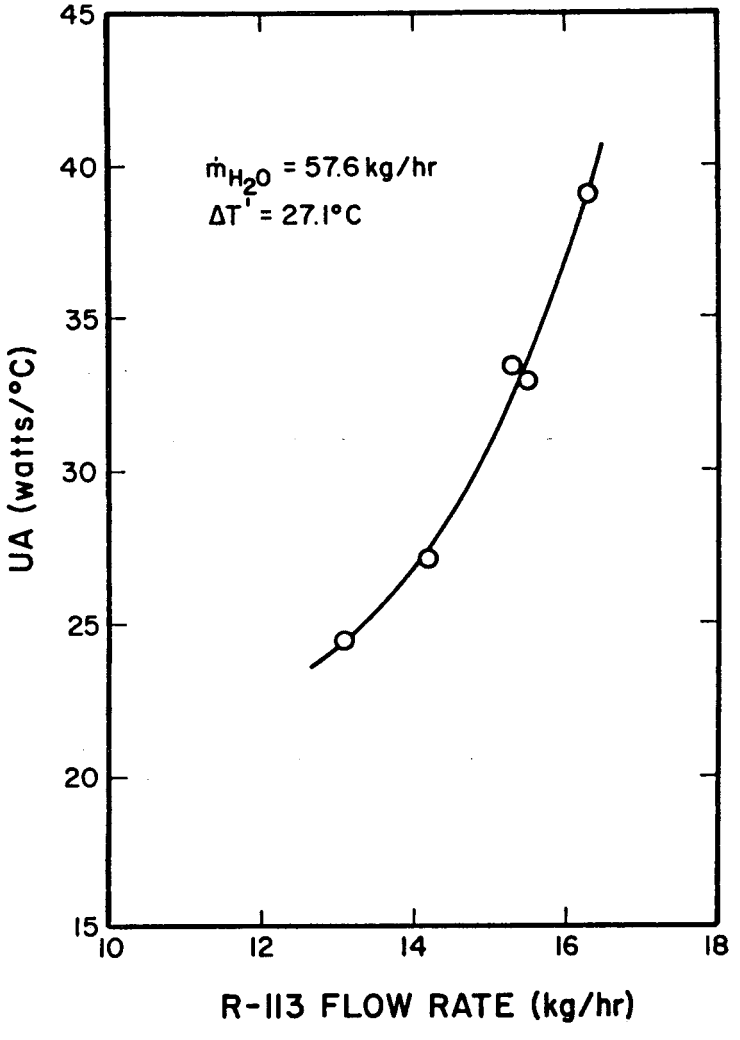

Figure 13. Effect of R-113 Flow Rate on UA Factor

appears to be unavoidable. Both Moore [8] and Sideman [1] have reported that for highly pure systems, drops of a volatile liquid suspended in an immiscible liquid medium required an extreme degree of superheat to initiate vaporization. In the system studied in this discussion, the large degree of turbulence and the impurities in the fluids produced minimum superheats of 5 to 7 °C. Figure 14 shows the degree of superheat as a function of water flow rate for various values of $\Delta T'$. The vertical bars crossing the curves in this figure represent the point at which buildup of R-113 began. Further tests with 6% by weight NaCl added to the water indicated negligible decrease in this superheat requirement, as shown by the solid circular symbols in Figure 14. Thus, further increases in the impurities in the water do not seem to appreciably further reduce the degree of superheat.

Another approach temperature that is useful in evaluating the performance of a direct contact heat exchanger is the pinch-point ΔT. This parameter is best described with the aid of Figure 15. Pinch-point ΔT is defined as the minimum vertical distance between the water curve and the R-113 curve. In all of the experiments carried out in this investigation, this minimum ΔT occurred between points A and B. Once again, one would like this parameter to be as small as possible in order to transfer as much of the available energy as possible. Figure 16 shows values for pinch-point ΔT calculated as a function of water flow rate for various values of $\Delta T'$. The vertical bars indicate points at which buildup begins to occur for the various

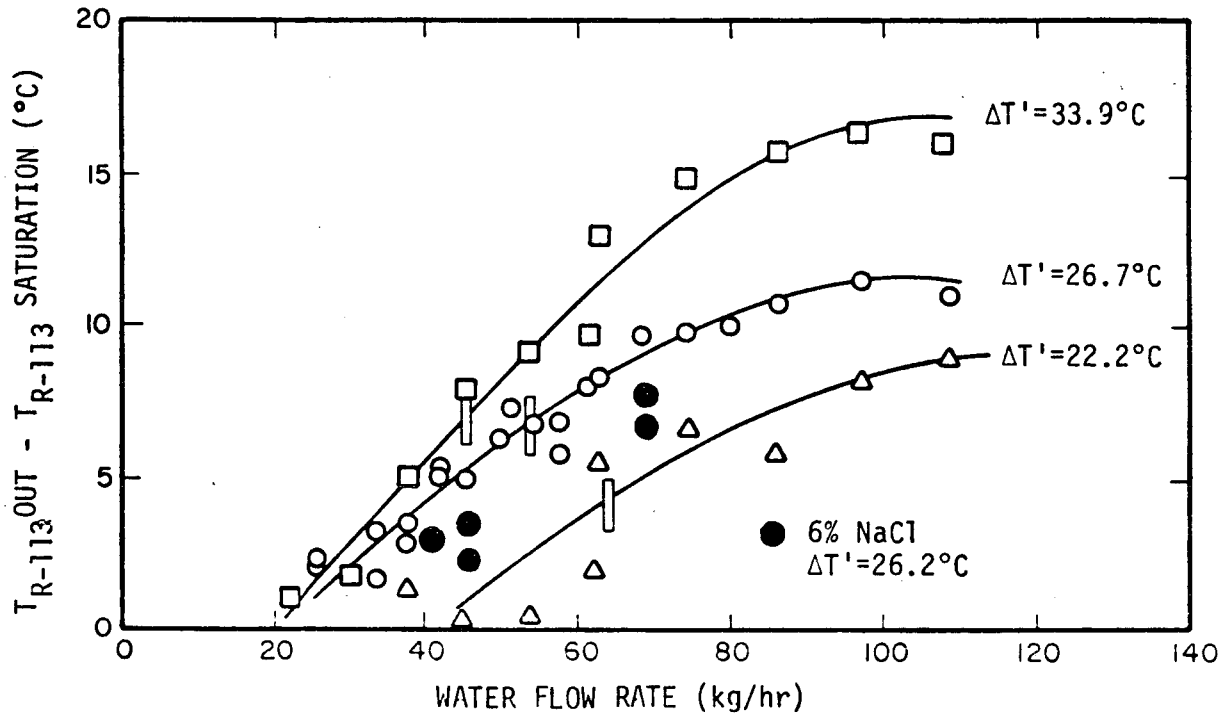

Figure 14. Effect of Water Flow Rate on R-113 Superheat

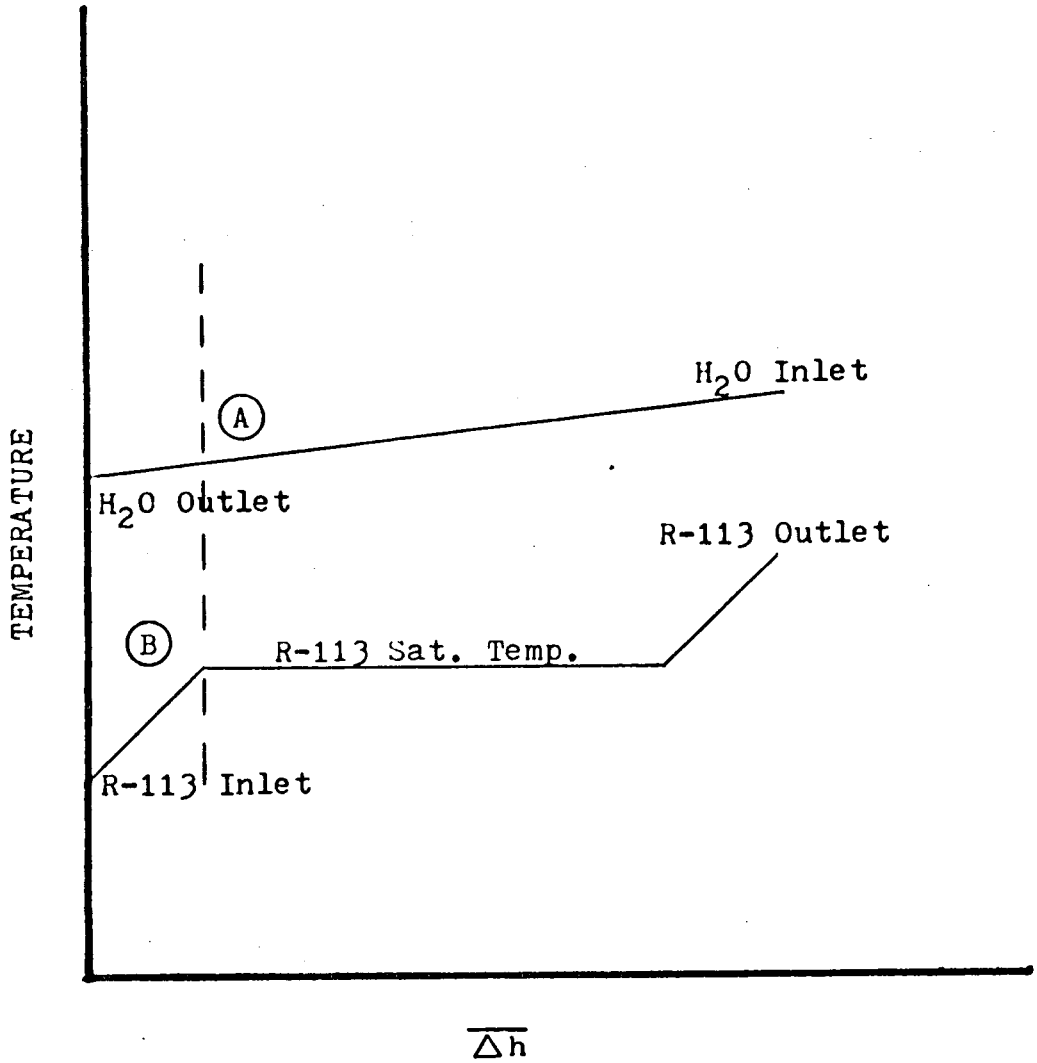

$$\overline{\Delta h} = \Delta h_{R\text{-}113} \quad \text{for R-113}$$

$$\overline{\Delta h} = (\dot{m}_{H_2O}/\dot{m}_{R\text{-}113})\Delta h_{H_2O} \quad \text{for water}$$

Figure 15. Pinch-point ΔT

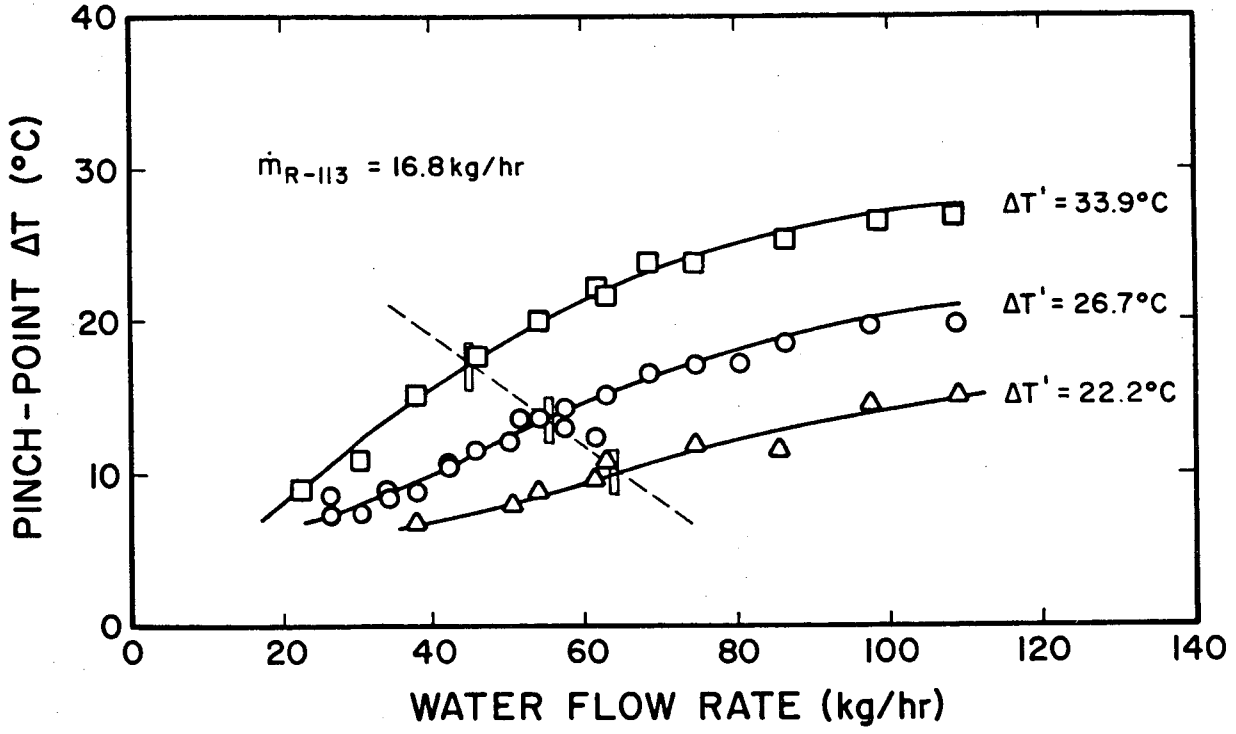

Figure 16. Effect of Water Flow Rate on Pinch-point ΔT

temperatures. For the range of conditions tested, the pinch-point ΔT appears to decrease linearly with increasing water flow rates. Minimum values for pinch-point ΔT are in the range of 10 to 15 °C.

D. Correlation Equation

Figure 17 represents an effort to correlate the heat transfer data from these experiments into a nondimensionalized equation. All data points used in this correlation were taken from the acceptable operating range where no buildup of R-113 was occurring. The nondimensionalized groups used to characterize the heat transfer for these data points are the following:

$$St = \frac{UA}{\dot{m}_{R\text{-}113} C_{P_{\ell}}{}_{R\text{-}113}}$$

$$H_{R\text{-}113} = Pr_{v_{R\text{-}113}} Ja_{v_{R\text{-}113}} = \frac{Pr_v h_{fg_{R\text{-}113}}}{C_{P_v} (T_{H_2O \text{ mean}} - T_{R\text{-}113 \text{ sat.}})}$$

and

$$\frac{\dot{m}_{\text{continuous phase}}}{\dot{m}_{\text{dispersed phase}}}$$

where St is the Stanton number, Pr is the Prandtl number, Ja is the Jakob number, C_p is the specific heat, and h_{fg} is the heat of vaporization. The temperature difference used in the Jakob number is the difference between the mean water temperature and the R-113 saturation temperature.

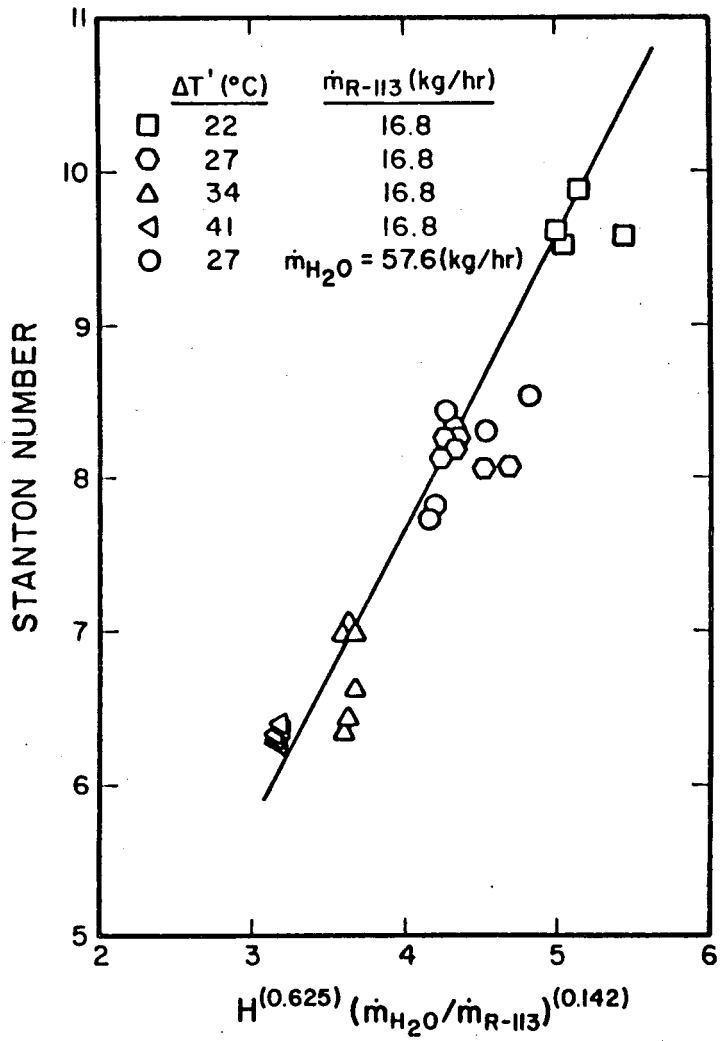

Figure 17. Nondimensional Heat Transfer for a Surface Type Boiler

The dimensionless group H comes from an analysis developed by Jacobs and Thomas [11], where it was noted that the important parameters for the evaporation of a single drop of a volatile fluid in a continuous liquid medium are the drop dimensions, velocity, the relative viscosities of the various fluids, the difference between the continuous phase fluid temperature and the saturation temperature of the volatile fluid. It was also shown, by developing an integral solution to the energy equation, that the product of the Prandtl number and the Jakob number based on the vapor properties of the dispersed phase (H) is proportional to the rate of evaporation of the liquid within the bubble. The recommended temperature difference used in the Jakob number was the difference between the temperature of the continuous phase and the saturation temperature of the volatile fluid.

The Stanton number was included in the correlation equation as a means of taking into account the strong dependence of the R-113 flow rate on the performance of the heat exchanger as demonstrated by Figure 13. It also has the advantage that no area term need be defined for the heat transfer process.

The final nondimensionalized parameter, the mass flow ratio, was included as a measure of the dispersion of the R-113 in the water. For the multiple drop problem, there is no clear dimension to characterize the flow; however, the ratio of initial drop diameter to drop spacing is obviously important since it affects both the ability of the drops to acquire heat from the continuous phase and the

coalescence of the drops. Since only one nozzle was used in the experiments, information concerning the ratio of drop diameter to drop spacing was not ascertained.

Using these three nondimensional groups, the correlation equation that best fits the data of Figure 13 is:

$$St = 1.91\ H^{(0.625)} \left(\frac{\dot{m}_{\text{continuous phase}}}{\dot{m}_{\text{dispersed phase}}} \right)^{(0.142)} \qquad (2)$$

V. CONCLUSIONS

The results obtained in this investigation can be summarized as follows:

1) Acceptable operating conditions are shown to be dependent on $\Delta T'$ and the mass flow ratio of water to R-113. Acceptable operating conditions are those conditions necessary to produce complete boiling of the R-113. It is shown that as $\Delta T'$ increases the required mass flow ratio decreases.

2) The efficiency of the heat exchanger, as described by the UA factor, is shown to have a strong dependence on $\Delta T'$. The UA factor drops rapidly as $\Delta T'$ increases for the range of temperatures tested in this study.

3) The UA factor is effectively independent of water flow rate as long as the flow is sufficiently high to produce complete boiling of the R-113.

4) The UA factor is strongly dependent on the R-113 flow rate. Increasing the R-113 flow rate results in a much higher UA factor.

5) The minimum approach temperatures, as described using the pinch-point ΔT, are shown to be in the range of 10 to 17 °C. This corresponds to minimum superheats of between 4 and 7 °C.

6) The Stanton number for heat transfer to the dispersed phase is shown to correlate with the product of the Jakob number and the Prandtl number, H. The correlation equation for the present experiment is:

$$St = 191\ H^{(0.625)}(\dot{m}_{H_2O}/\dot{m}_{R\text{-}113})^{(0.142)}$$

for conditions where buildup does not occur.

LIST OF REFERENCES

1. Sideman, S. and Taitel, Y., "Direct Contact Heat Transfer with Change of Phase: Evaporation of Drops in an Immiscible Liquid Medium," International Journal of Heat and Mass Transfer, Vol. 7, pp. 1273-1289, 1964.

2. Wiegandt, H. F., Office of Saline Water Progress Report No. 41, August 1960.

3. Karnofsky, G. and Steinhoff, P. F., Office of Saline Water Progress Report No. 40, July 1960.

4. Shiloh, K. and Sideman, S., "Direct Contact Heat Transfer with Changer of Phase: Evaporation Rates in Vacuum Freezers," The Canadian Journal of Chemical Engineering, Vol. 45, pp. 300-305, October 1967.

5. Wilke, C. R., Chang, C. T., Ledesma, V. L. and Porter, J. W., "Direct Contact Heat Transfer for Sea Water Evaporation," Chemical Engineering Progress, Vol. 59, No. 12, pp. 69-75, December 1963.

6. Boehm, R. F. and Jacobs, H. R., "Feasibility Study of the Application of Direct Contact Heat Exchangers to Power Cycles Utilizing Geothermal Brines," Energy Research and Development Administration, E-(11-1)2601, July 1974.

7. Blander, M., Hengstenberg, D. and Katz, J. L., "Bubble Nucleation in n-Pentane, n-Hexane, n-Pentane + Hexadecane Mixtures, and Water," The Journal of Physical Chemistry, Vol. 75, No. 23, pp. 3613-3619, 1971.

8. Moore, G. R., "Vaporization of Superheated Drops in Liquids," AIChE Journal, Vol. 5, No. 4, pp. 458-466, December 1959.

9. Simpson, H. C., Beggs, G. C. and Nazir, M., "Evaporation of Butane Drops in Brine," 4th International Symposium on Fresh Water From the Sea, Heidelberg, Vol. 3, pp. 409-420, 1973.

10. Simpson, H. C., Beggs, G. C. and Nazir, M., "Evaporation of a Droplet of One Liquid Rising Through a Second Immiscible Liquid - A New Theory of the Heat Transfer Process," Fifth International Heat Transfer Conference, 1974.

11. Jacobs, H. R. and Thomas, K. D., "Evaporation of Immiscible Drops Within a Continuous Media," UTEC ME 75-111, University of Utah, 1975.

12. Waldram, K. L., Fauske, H. K. and Bankoff, S. G., "Impaction of Volatile Liquid Droplets Onto a Hot Liquid Surface," 15th National Heat Transfer Conference, San Francisco, Calif., August 1975.

13. Sideman, S. and Gat, Y., "Direct Contact Heat Transfer with Change of Phase: Spray Column Studies of a Three Phase Heat Exchanger," AIChE Journal, Vol. 12, No. 3, pp. 296-303, March 1966.

14. Somer, T. G., Bora, M., Kaymakcalan, O., Ozmen, S. and Arikan, Y., "Heat Transfer to an Immiscible Liquid Mixture and Between Liquids in Direct Contact," Desalination, Vol. 13, pp. 231-249, 1973.

15. Somer, T. G., Bora, M., Kaymakcalan, O., Ozmen, S. and Arikan, Y., "Pilot Plant Study of Desalination by Direct Contact Heat Transfer," Desalination, Vol. 13, pp. 221-229, 1973.

16. Drake, E. M., Jeje, A. E. and Reid, R. C., "Transient Boiling of Liquefied Cryogens on a Water Surface I. Nitrogen, Methane and Ethane," International Journal of Heat and Mass Transfer, Vol. 18, pp. 1361-1368, 1975.

17. Drake, E. M., Jeje, A. E. and Reid, R. C., "Transient Boiling of Liquefied Cryogens on a Water Surface II. Light Hydrocarbon Mixtures," International Journal of Heat and Mass Transfer, Vol. 18, pp. 1369-1375, 1975.

18. Marshall, W. R., Atomization and Spray Drying, American Institute of Chemical Engineers, New York, New York, 1954.

19. Keenan, J. H., Keyes, F. G., Hill, P. G. and Moore, J. G., Steam Tables, New York, New York, John Wiley & Sons, Inc., 1969.

20. Thermodynamic Properties of Refrigerants, New York, New York, ASHRAE, 1969.

APPENDIX I

HEAT LOSS FROM VESSEL

Heat loss from the vessel was calculated by reducing the vessel to a composite flat plate with a surface area equal to that of the vessel. The total surface area of the various materials used in the construction of the vessel is given below:

Material	Area	Thermal Conductivity
5/8" mild steel	0.539 m^2	44 watts/m °C
1" mild steel	0.045 m^2	44 watts/m °C
3/16" tempered glass	0.260 m^2	0.76 watts/m °C

The entire vessel was insulated using three inches of polyurethane foam with a thermal conductivity of 0.032 watts/m °C. The internal heat transfer coefficient was assumed to be 60 watts/m^2 °C and the external heat transfer coefficient was assumed to be 30 watts/m^2 °C. The temperature within the vessel was taken as 75 °C and room temperature was assumed to be 23 °C. Using these assumptions, the following heat losses were calculated:

Material	Heat Loss
5/8" mild steel + insulation	11 watts
1" mild steel + insulation	1 watt
3/16" tempered glass + insulation	4 watts
Total	16 watts

Typical values of heat transferred from the water to the R-113 were on the order of 800 watts. This means that the heat loss from the vessel to the environment was a mere 2% of the heat being transferred. This is well below the range of what can be accurately measured and therefore was neglected in the heat balance calculations.

APPENDIX II

DATA REDUCTION

The data obtained from the experimental apparatus used in this investigation consisted of the temperature at the water inlet (T_{wi}), the temperature at the water outlet (T_{wo}), the temperature at the R-113 inlet (T_{Ri}), the temperature at the R-113 outlet (T_{Ro}), the flow rates of the water ($\dot{m}_w$) and the R-113 ($\dot{m}_R$), vessel pressure (P_v), and atmospheric pressure (P_a). This data was reduced to give values for the net heat lost from the water (Q_w), the net heat gained by the R-113 (Q_R), the UA factor (UA), and the pinch-point ΔT (ΔT_p).

Heat Balance

The heat balance for the test vessel was obtained utilizing the following assumptions:

1) All of the R-113 entering the vessel was vaporized and left the vessel through the R-113 outlet line.
2) A portion of the water entering the vessel was vaporized and left the vessel through the R-113 outlet line as saturated vapor at the R-113 outlet temperature.
3) Heat losses to the environment were assumed negligible.

These assumptions lead to the energy equation shown below:

$$\dot{m}_{wl}(h_{wi}-h_{wo}) + \dot{m}_s(h_{wi}-h_{so}) + \dot{m}_R(h_{Ri}-h_{Ro}) = 0 \qquad \text{(II-1)}$$

where $\dot{m}_{wl}$ is that portion of the water entering the vessel that remains in the liquid state, $\dot{m}_s$ is that portion of the water entering the vessel that is vaporized, $\dot{m}_R$ is the R-113 flow rate, and h_{wi}, h_{wo}, h_{so}, h_{Ri} and h_{Ro} are the respective enthalpies of the water in, the water out, the steam out, the R-113 in and the R-113 out.

The mass flow rate of the R-113 can be obtained directly from the experimental data; however, $\dot{m}_{wl}$ and $\dot{m}_s$ must be calculated. Letting P_s equal the partial pressure of the water vapor in the vessel, P_R equal the partial pressure of the R-113 vapor in the vessel, and using the definition of partial pressure:

$$\frac{P_s}{P_R} = \frac{\dot{m}_s M_R}{\dot{m}_R M_s} \qquad \text{(II-2)}$$

where M_R and M_w are the molecular weights of R-113 and water respectively. Reducing this equation gives:

$$\dot{m}_s = \frac{\dot{m}_R M_w P_s}{M_R P_R} \qquad \text{(II-3)}$$

P_s can be found in steam tables as the saturation pressure for a temperature of T_{Ro} and P_R can be calculated from the equation

$P_R = P_v - P_s$, thus yielding $\dot{m}_s$. $\dot{m}_{wl}$ can now be calculated using $\dot{m}_{wl} = \dot{m}_w - \dot{m}_s$.

Now that the flow rate in Equation (II-1) have been obtained, determination of the enthalpy change can be made. The enthalpy change of the water that remains liquid can be directly found using the definition of specific heats, i.e., $c_p \Delta T = \Delta h$. This reduces Equation (II-1) to:

$$\dot{m}_{wl} c_{p_w} (T_{wi} - T_{wo}) + \dot{m}_s (h_{wi} - h_{so}) + \dot{m}_R (h_{Ri} - h_{Ro}) = 0 \qquad \text{(II-4)}$$

The portion of the water flow being vaporized enters the vessel and gives up heat as its temperature drops from T_{wi} to T_{Ro}. It then evaporates, absorbing an amount of heat equal to its heat of vaporization (h_{fg_w}) at the temperature of T_{Ro}. The net enthalpy change for the water that vaporizes is thus:

$$h_{wi} - h_{so} = c_{p_w} (T_{wi} - T_{Ro}) - h_{fg_w} \qquad \text{(II-5)}$$

Substituting into Equation (II-4) gives:

$$m_{wl} c_{p_w} (T_{wi} - T_{wo}) + m_s \left[c_{p_w} (T_{wi} - T_{Ro}) - h_{fg_w} \right] + m_R (h_{Ri} - h_{Ro}) = 0 \qquad \text{(II-6)}$$

The enthalpy change of the R-113 can be broken up into three parts. First the liquid R-113 entering is heated up to its saturation temperature, absorbing an amount of heat equal to $c_{P_R} (T_{R_{sat}} - T_{Ri})$,

where $T_{R_{sat}}$ is the saturation temperature of the R-113 at a pressure of P_R. The R-113 is then vaporized, absorbing an amount of heat equal to h_{fg_R}, where h_{fg_R} is the heat of vaporization of R-113 at a pressure of P_R. Finally, the R-113 vapors are superheated absorbing an amount of heat given by $h_{s_R} - h_{g_R}$ where h_{s_R} is equal to the enthalpy of the superheated vapors at T_{Ro} and h_{g_R} is equal to the enthalpy of the saturated vapors at $T_{R_{sat}}$. Substituting these values into Equation (II-6) gives the final energy balance:

$$\dot{m}_{wl} c_{p_w} (T_{wi} - T_{wo}) + \dot{m}_s \left[c_{p_w} (T_{wi} - T_{Ro}) - h_{fg_w} \right]$$

$$+ \dot{m}_R \left[c_{p_R} (T_{Ri} - T_{R_{sat}}) - h_{fg_R} + (h_{s_R} - h_{g_R}) \right] = 0 \qquad \text{(II-7)}$$

Values for the properties of water were obtained from Reference [19] and values for the properties of R-113 were obtained from Reference [20].

Rearranging Equation (II-7) yields:

$$\dot{m}_{wl} c_{p_w} (T_{wi} - T_{wo}) + \dot{m}_s \left[c_{p_w} (T_{wi} - T_{so}) - h_{fg_w} \right] =$$

$$\dot{m}_R \left[c_{P_R} (T_{R_{sat}} - T_{Ri}) + h_{fg_R} + (h_{s_R} - h_{g_R}) \right] \qquad \text{(II-8)}$$

The left side of this equation represents the net heat transferred from the water (Q_w) and the right side of this equation represents the net heat transferred to the R-113 (Q_R). Thus, the definitions of

Q_w and Q_R are:

$$Q_w = m_{wl} c_{p_w} (T_{wi} - T_{wo}) + m_s \, c_{p_w} (T_{wi} - T_{R_o}) - h_{fg_w} \qquad \text{(II-9)}$$

$$Q_R = \dot{m}_R \, c_{P_R} (T_{R_{sat}} - T_{Ri}) + h_{fg_R} + (h_{s_R} - h_{g_R}) \qquad \text{(II-10)}$$

UA Factor

The UA factor was defined as the net heat transferred divided by the log mean temperature difference assuming counter-current flow.

$$UA = \frac{Q_R}{LMTD} \qquad \text{(II-11)}$$

where

$$LMTD = \frac{\Delta T_a - \Delta T_b}{\ln(\Delta T_a / \Delta T_b)}$$

and

$$\Delta T_a = T_{wi} - T_{Ro}$$

$$\Delta T_b = T_{wo} - T_{Ri}$$

Pinch-point ΔT (ΔT_p)

Pinch-point ΔT was calculated with the aid of Figure 18. The equation for the water curve (line AB) can be shown to be:

$$T - T_{wo} = \left[\frac{T_{wi} - T_{wo}}{\overline{\Delta h_1}}\right](\overline{\Delta h}) \qquad \text{(II-13)}$$

The pinch-point ΔT is defined as the minimum vertical distance between the water curve and the R-113 curve. This occurs between points C and D in Figure 18. The value of $\overline{\Delta h}$ at these points can be calculated from the R-113 curve. $\overline{\Delta h_2}$ is equal to the change in enthalpy associated with the heating of the liquid R-113 from entrance conditions to saturation conditions as calculated from the equation:

$$\overline{\Delta h_2} = c_{p_R}(T_{R_{sat}} - T_{Ri}) \qquad \text{(II-14)}$$

The temperature of the R-113 at point C is the saturation temperature of the R-113.

The temperature at point D on the water curve can now be calculated from Equation (II-13).

$$T_{wp} = \left[\frac{T_{wi} - T_{wo}}{\overline{\Delta h_1}}\right]\overline{\Delta h_2} + T_{wo} \qquad \text{(II-15)}$$

Multiplying the right side by $\frac{\dot{m}_w c_{p_w} \dot{m}_R}{\dot{m}_w c_{p_w} \dot{m}_R}$ gives:

$$T_{wp} = \frac{m_w c_{p_w}(T_{wi} - T_{wo}) m_R \; h_2}{(\dot{m}_R \; h_1)\dot{m}_w c_{p_w}} + T_{wo}$$

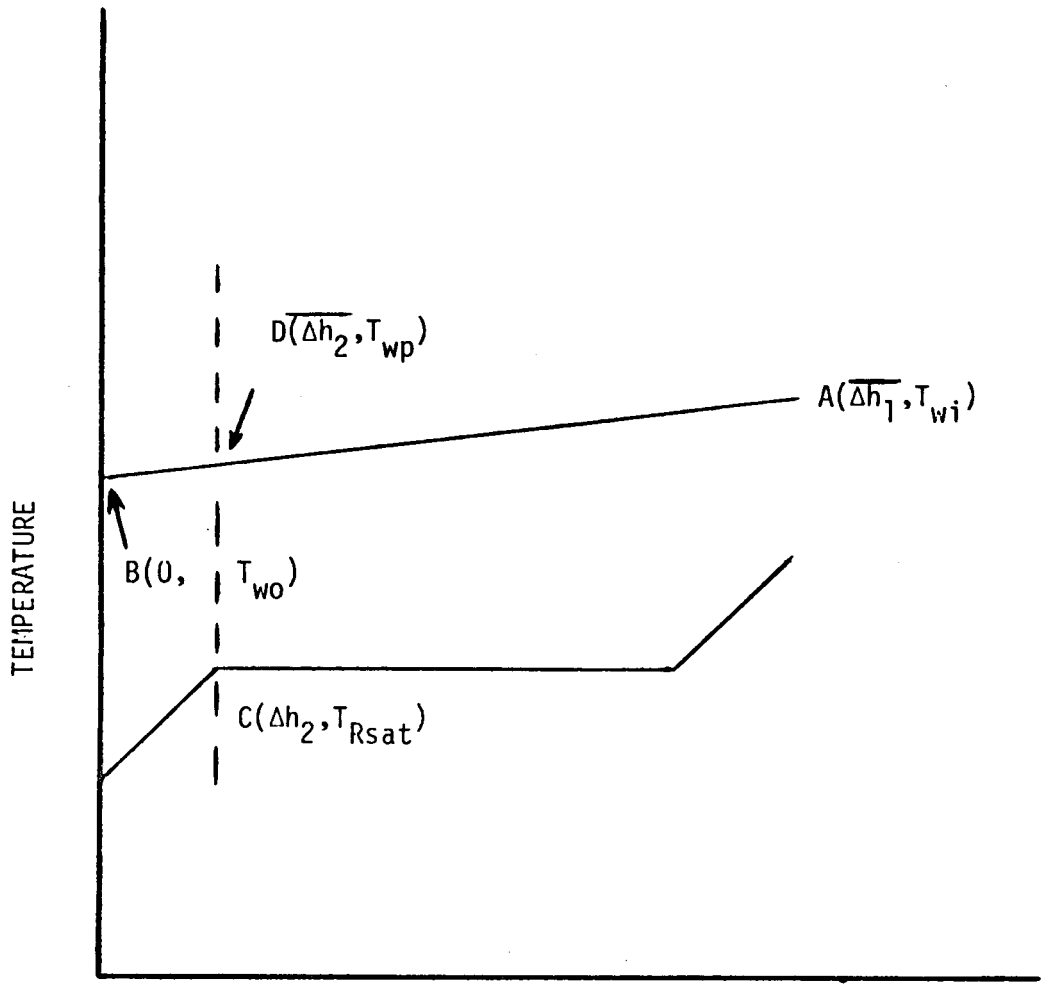

$\overline{\Delta h} = \Delta h_{R\text{-}113}$ for R-113

$\overline{\Delta h} = (\dot{m}_{H_2O}/\dot{m}_{R\text{-}113})\Delta h_{H_2O}$ for water

Figure 18. Pinch-point ΔT

which reduces to:

$$T_{wp} = \frac{Q_w Q_{R1}}{Q_R \dot{m}_w c_{p_w}} + T_{wo} \qquad \text{(II-16)}$$

where Q_{R1} is the energy added to the R-113 to heat it from entrance conditions to saturation conditions. Since the net energy added to the R-113 is equal to the net energy lost from the water, Equation (II-16) reduces to:

$$T_{wp} = \frac{Q_{R1}}{\dot{m}_w c_{p_w}} + T_{wo} \qquad \text{(II-17)}$$

The pinch-point ΔT can now be directly calculated by:

$$\Delta T_p = T_{wp} - T_{R_{sat}} \qquad \text{(II-18)}$$

or

$$\Delta T_p = \frac{Q_{R1}}{\dot{m}_w c_{p_w}} + T_{wo} - T_{R_{sat}} \qquad \text{(II-19)}$$

Nomenclature for Appendix II

c_{p_R} - Liquid specific heat of R-113

c_{p_w} - Liquid specific heat of water

h_{fg_R} - R-113 heat of vaporization

h_{fg_w} - Water heat of vaporization

h_{Ri} - Enthalpy of R-113 entering vessel

h_{Ro} - Enthalpy of R-113 leaving vessel

h_{gR} - Enthalpy of saturated R-113 vapors

h_{wi} - Enthalpy of water entering vessel

h_{wo} - Enthalpy of water leaving vessel

h_{so} - Enthalpy of steam leaving vessel

Δh_1 - Total enthalpy change of R-113

Δh_2 - Enthalpy change associated with the heating of the liquid R-113 from inlet conditions to saturation conditions

LMTD - Log mean temperature difference

$\dot{m}_R$ - Mass flow rate of R-113

$\dot{m}_s$ - Mass flow rate of water turning to steam

$\dot{m}_w$ - Total flow rate of water

$\dot{m}_{wl}$ - Mass flow rate of water remaining liquid

M_R - Molecular weight of R-113

M_w - Molecular weight of R-113

P_a - Atmospheric pressure

P_R - Partial pressure of R-113 in vessel

P_s - Partial pressure of water vapor in vessel

P_v - Vessel pressure

Q_R - Net heat gained by R-113

Q_{R1} - Energy added to the R-113 to heat it from entrance conditions to saturation conditions

T_{Ri} - R-113 inlet temperature

T_{Ro} - R-113 outlet temperature

$T_{R_{sat}}$ - R-113 saturation temperature

T_{wi} - Water inlet temperature

T_{wo} - Water outlet temperature

T_{wp} - Temperature of water used in calculating ΔT_p

ΔT_p - Pinch-point ΔT

APPENDIX III

COMPUTER ROUTINE

This discussion contains instructions for the operation of the data reduction routine, the necessary inputs, a variable list, a listing of the program, and a sample output. The program was written in the Real Time Basic language using the Univac 1108 computer at the University of Utah Computing Center.

The inputs to the program are:

1. The thermocouple readings of the water inlet, the water outlet, the R-113 inlet, and the R-113 outlet, all in millivolts.
2. The flow meter number (1 for the high range flow meter or 2 for the low range flow meter) and the flow meter reading for the water side.
3. The R-113 flow rate in gallons per hour.
4. Tank pressure and atmospheric pressure in inches of mercury.

The computer utilizes a series of curve fits to convert these inputs into their various values.

List of Variables

D1 - LMTD (°F)

D2 - Intermediate temperature

D3 - Intermediate temperature

D4 - R-113 flow rate (kg/hr)

D5 - Flow rate of water leaving vessel as steam (kg/hr)

D6 - Flow rate of water leaving vessel as liquid (kg/hr)

D7 - LMTD (°C)

D8 - R-113 saturation temperature (°C)

F1 - Total water flow rate (gal/hr)

F2 - R-113 flow rate (gal/hr)

F5 - Total water flow rate (lbm/hr)

F6 - R-113 flow rate (lbm/hr)

F7 - Flow rate of water leaving vessel as steam (lbm/hr)

F8 - Flow rate of water leaving vessel as liquid (lbm/hr)

F9 - Total water flow rate (kg/hr)

H1 - Enthalpy of saturated R-113 liquid (Btu/lbm)

H2 - Enthalpy of saturated R-113 vapor (Btu/lbm)

H3 - R-113 heat of vaporization (Btu/lbm)

H4 - Enthalpy of superheated R-113 (Btu/lbm)

H7 - Water heat of vaporization (Btu/lbm)

K1 - Water flow meter number

P1 - Vessel pressure (inches mercury gage)

P2 - Atmospheric pressure (inches mercury)

P3 - Partial pressure of R-113 in vessel (psi)

P4 - Intermediate pressure

P5 - Partial pressure of water in vessel (Pa)

P6 - Partial pressure of R-113 in vessel (Pa)

P7 - Partial pressure of water in vessel (psi)

P8 - Vessel pressure (psia)

P9 - Vessel pressure (Pa)

Q1 - Heat transferred from water ($mc_p\Delta T$) (Btu/hr)

Q2 - Total heat transferred to R-113 (Btu/hr)

Q5 - Heat transferred to heat liquid R-113 to saturation (Btu/hr)

Q6 - Heat transferred to evaporate R-113 (Btu/hr)

Q7 - Heat transferred to superheat R-113 (Btu/hr)

S - Intermediate number

S1 - Pinch-point ΔT (°F)

S2 - Pinch point ΔT (°C)

S5 - Mean water temperature (°F)

S6 - Mean water temperature (°C)

T1 - Water inlet temperature (°F)

T2 - Water outlet temperature (°F)

T3 - R-113 inlet temperature (°F)

T4 - R-113 outlet temperature (°F)

T5 - Water inlet temperature (°C)

T6 - Water outlet temperature (°C)

T7 - R-113 inlet temperature (°C)

T8 - R-113 outlet temperature (°C)

T9 - R-113 saturation temperature (°F)

U - UA factor (Btu/hr °F)

U1 - Heat loss from water that remains liquid (Btu/hr)

U2 - Heat taken by water turning to steam (Btu/hr)

U3 - Net heat transferred from water (Btu/hr)

U4 - UA factor (watts/°C)

W1 - Heat transferred to heat liquid R-113 to saturation (watts)

W2 - Heat transferred to evaporate R-113 (watts)

W3 - Heat transferred to superheat R-113 (watts)

W4 - Total heat transferred to R-113 (watts)

W5 - Heat loss from water that remains liquid (watts)

W6 - Heat taken by water turning to steam (watts)

W7 - Net heat transferred from water (watts)

Program List

```
100 PRINT 'INPUT THE MILLIVOLT READINGS FOR: 1)TEMP. WATER IN'
105 '2) TEMP. WATER OUT 3) TEMP. R-113 IN 4) TEMP.'
110 PRINT 'R-113 OUT.'
115 INPUT T1,T2,T3,T4
120 REM CALCULATE TEMPERATURES FROM CALIBRATION CURVE FITS (F)
125 LET T1=-.6379795*T1*T1+45.69303*T1+33.23435
130 LET T2=-.4946314*T2*T2+45.21539 T2+33.65707
135 LET T3=-.4719833*T3*T3+45.17156*T3+33.61337
140 LET T4=-.2423911*T4*T4+44.14771*T4*34.56679
145 LET S5 =(T1+T2)/2
150 REM  CONVERT TEMPERATURES TO C
155 LET A=.55488
160 LET B=17.755
165 LET T5=A*T1-B
170 LET T6=A*T2-B
175 LET T7=A*T3-B
180 LET T8=A*T4-B
185 LET S6=A*S5-B
190 PRINT 'INPUT FLOW METER # AND READING FOR WATER'
195 INPUT K1,F1
200 REM  CALCULATE WATER FLOW RATE FROM CALIBRATION CURVE
205 REM  FITS IN GPH
210 IF K1=1 THEN 225
220 GO TO 235
225 LET F1 =1.553*F1-3.230
230 REM  CONVERT WATER FLOW RATE TO LBM/HR AND KG/HR
235 LET F5=8.1813*F1
240 LET F9=F5/2.205
245 PRINT 'INPUT R-113 FLOW RATE (GPH)'
250 INPUT F2
255 REM  CALCULATE R-113 FLOW RATE IN LBM/HR AND KG/HR
260 LET F6=12.962*F2
265 LET D4=F6/2.205
270 PRINT 'INPUT TANK P AND ATMOS. P (IN. HG.)'
275 INPUT P1,P2
280 LET P8=.49118*(P1+P2)
285 LET P9=6894*P8
290 REM  CALCULATE PARTIAL PRESSURE OF WATER VAPOR IN VESSEL
295 REM  (PSI AND PA) AND THE ASSOCIATED HEAT OF VAPORIZATION
300 REM  (BTU/LBM) FROM STEAM TABLE CURVE FITS.
305 IF T4<100 THEN 320
310 IF T4<131 THEN 330
315 IF T4<162 THEN 345
320 PRINT 'TEMP. R-113 OUT EXCEEDS STEAM TABLE CURVE FIT'
325 GO TO 1155
330 LET P7=.5101799E-3*T4*T4-.7508953E-1*T4+3.36946
335 LET H7=-.9704596E-4*T4*T4-.5514279*T4+1093.1
```

```
340 GO TO 355
345 LET P7=.9218157E-3*T4*T4-.1837579*T4+10.54667
350 LET H7=-.2485435E-3*T4*T4-.5141338*T4+1090.82
355 LET P5=6894*P7
360 REM  CALCULATE PARTIAL PRESSURE R-113 IN PSI AND PA
365 LET P3=P8-P7
370 LET P6=6894*P3
375 REM  CALCULATE STEAM CARRYOVER IN LBM/HR AND KG/HR
380 LET F7=(.096056*F6*P7)/P3
385 LET D5=F7/2.205
390 REM  CALCULATE FLOW RATE OF WATER LEAVING THE VESSEL
395 REM  AS LIQUID IN LBM/HR AND KG/HR
400 LET F=F5-F7
405 LET D6=F8/2.205
410 REM  CALCULATION OF Q FOR R-113 USING A LIQUID DENSITY OF
415 REM  96.96 LBM PER CUBIC FOOT AND A SPECIFIC HEAT OF THE
420 REM  LIQUID OF .218 BTU PER LBM PER DEGREE F
425 REM
430 REM  CALCULATE R-113 SATURATION TEMPERATURE (F AND C),
435 REM  LIQUID ENTHALPY (BTU/LBM), AND VAPOR ENTHALPY (BTU/LBM)
440 REM  FROM R-113 TABLE CURVE FITS.
445 IF P3<10.5 THEN 470
450 IF P3<14.5 THEN 480
455 IF P3<19.5 THEN 500
460 IF P3<25.5 THEN 520
465 IF P3<30.5 THEN 540
470 PRINT 'PRESSURE EXCEEDS RANGE OF R-113 TABLE CURVE FIT'
475 GO TO 1125
480 LET T9=-.1250575*P3*P3+7.293981*P3+37.30327
485 LET H1=-.2576664E-1*P3*P3+1.576661*P3+15.30357
490 LET H2=-.1840998E-1*P3*P3+1.076896*P3+84.19097
495 GO TO 555
500 LET T9=-.7635257E-1*P3*P3+5.870781*P3+47.70107
505 LET H1=-.1539114E-1*P3*P3+1.267993*P3+17.59979
510 LET H2=-.1145736E-1*P3*P3+.8718381*P3+85.70316
515 GO TO 555
520 LET T9=-.4843597E-1*P3*P3+4.815339*P3+57.68259
525 LET H1=-.1026264E-1*P3*P3+1.073061*P3+19.45455
530 LET H2=-.745658E-2*P3*P3+.7225737*P3+87.09507
535 GO TO 555
540 LET T9=-.3106334E-1*P3*P3+3.970668*P3+67.92628
545 LET H1=-.5800642E-2*P3*P3+.8499256*P3+22.24455
550 LET H2=-.4097026#-2*P3*P3+.5567701*P3+89.13838
555 LET D8=(T9-32)/1.8
560 REM  CALCULATE R-113 HEAT OF VAPORIZATION (BTU/LBM).
565 LET H3=H2-H1
570 REM  CALCULATE ENTHALPY OF SUPERHEATED R-113 VAPOR LEAVING
575 REM  THE VESSEL (BTU/LBM) USING R-113 TABLE CURVE FIT.
580 LET H4=.56745E-4*T4*T4+.1449534*T4+78.18323
585 LET P4=16-P4
```

```
590 LET H4=H4+.04*P4
595 REM  CALCULATE HEAT ADDED TO R-113 TO HEAT IT TO SATURATION
600 REM  (BTU/HR), TO BOIL IT (BTU/HR), TO SUPERHEAT IT (BTU/HR),
605 REM  AND THE TOTAL HEAT ADDED (BTU/HR).
610 LET Q5=.218*F6*(T9-T3)
615 LET Q6=F6*H3
620 LET Q7=F6*(H4-H2)
625 LET Q2=Q5+Q6+Q7
630 REM  CONVERT THESE VALUES TO WATTS.
635 LET A=3.413
640 LET W1=Q5/A
645 LET W2=Q6/A
650 LET W3=Q7/A
655 LET W4=Q2/A
660 REM  CALCULATION OF Q FOR WATER SIDE (BTU/HR AND WATTS)
665 REM  USING A LIQUID DENSITY OF 61.2 LBM/CUBIC FOOT
670 REM  AND A LIQUID SPECIFIC HEAT OF 1.0 BTU/LBM F.
675 LET U1=F8*1.0*(T1-T2)
680 LET U2=F7*(H7-(1.0*(T1-T4)))
685 LET U3=U1-U2
690 LET W6=U1/3.413
695 LET W6=U2/3.413
700 LET W7=U3/3.413
705 REM  CALCULATION LMTD (F AND C) ASSUMING A COUNTERFLOW
710 REM  CONFIGURATION
715 LET D2=T1-T4
720 LET D3=T2-T3
725 LET D1=(D2-D3)/(LOG(D2/D3))
730 LET D7=D1/1.8
735 REM  CALCULATION OF UA FACTOR (BTU/HR F AND WATTS/C)
740 LET U=Q2/D1
745 LET U4=U*.5274
750 REM  CALCULATION OF PINCH-POINT DELTA T (F AND C)
755 LET S=(Q5/(8.18125*F1))+T2
760 LET S1=S-T9
765 LET S2=S1/1.8
770 REM  OUTPUT
775 PRINT
780 PRINT
785 PRINT 'TEMP. WATER IN ='T1,'F',T5,'C'
790 PRINT 'TEMP. WATER OUT ='T2,'F',T6,'C'
795 PRINT 'TEMP. R-113 IN ='T3,'F',T7,'C'
800 PRINT 'TEMP. R-113 OUT ='T4,'F',T8,'C'
805 PRINT
810 PRINT 'R-113 SAT. TEMP. ='T9,'F',D8,'C'
815 PRINT
820 PRINT 'MEAN WATER TEMP ='S5,'F',S6,'C'
825 PRINT
830 PRINT
835 PRINT 'TOTAL WATER FLOW RATE =',F5,'LBM/HR'
```

```
840 PRINT ,,F9,'KG/HR'
845 PRINT
850 PRINT 'WATER FLOW REMAINING LIQUID =',F5,'LBM/HR'
855 PRINT ,,D6,'KG/HR'
860 PRINT
865 PRINT 'WATER FLOW LEAVING AS STEAM =',F7,'LBM/HR'
870 PRINT ,,D5,'KG/HR'
875 PRINT
880 PRINT
885 PRINT
890 PRINT 'R-113 FLOW RATE ='F6,'LBM/HR',D4,'KG/HR'
895 PRINT
900 PRINT
905 PRINT
910 PRINT 'TANK PRESSURE =',P8,'PSIA'
915 PRINT ,, P9,'PA'
920 PRINT
925 PRINT 'PARTIAL PRESSURE STEAM =',P7,'PSI'
930 PRINT ,,P5,'PA'
935 PRINT
940 PRINT 'PARTIAL PRESSURE R-113 =',P3,'PSI'
945 PRINT ,,P6,'PA'
950 PRINT
955 PRINT
960 PRINT
965 PRINT 'HEAT LOSS FROM WATER REMAINING LIQUID =',U1,'BTU/HR'
970 PRINT ,,,W5,'WATTS'
975 PRINT
980 PRINT 'HEAT GAIN FROM WATER TURNING TO STEAM =',U2,'BTU/HR'
990 PRINT
995 PRINT 'NET HEAT TRANSFERRED FROM WATER ='U3,'BTU/HR'
1000 PRINT ,,,,W7,'WATTS'
1005 PRINT
1010 PRINT
1015 PRINT
1020 PRINT 'HEAT ADDED TO LIQUID R-113 =',,Q5,'BTU/HR'
1025 PRINT ,,, W1,'WATTS'
1030 PRINT
1035 PRINT 'HEAT ADDED TO BOIL R-113 =',,Q6,'BTU/HR'
1040 PRINT ,,, W2,'WATTS'
1045 PRINT
1050 PRINT 'HEAT ADDED TO SUPERHEAT R-113 =',Q7,'BTU/HR'
1055 PRINT ,,,,W3,'WATTS'
1060 PRINT
1065 PRINT 'NET HEAT ADDED TO R-113 =',,Q2,'BTU/HR'
1070 PRINT ,,,W4,'WATTS'
1075 PRINT
1080 PRINT
1085 PRINT
```

```
1090 PRINT 'LMTD =',D1,'F;,D7,'C'
1095 PRINT
1100 PRINT
1105 PRINT 'UA =',U,'BTU/LBM F',U4,'WATTS/C'
1110 PRINT
1115 PRINT
1120 PRINT 'PINCH-POINT =',S1,'F',S2,'C'
1125 PRINT
1130 PRINT
1135 PRINT
1140 PRINT
1145 PRINT
1150 GO TO 100
1155 END
>
```

Sample Output

```
RUNNH


INPUT THE MILLIVOLT READINGS FOR:  1:TEMP. WATER IN
2) TEMP. WATER OUT  3) TEMP. R-113 IN 4) TEMP.
R-113 OUT.
? 3.106,2.754,1.267,2.320
INPUT FLOW METER # AND READING FOR WATER
? 1,21
INPUT R-113 FLOW RATE (GPH)
? 2.893
INPUT TANK P AND ATMOS. P (IN. HG.)
? 4.25,25.42


TEMP. WATER IN = 169.00216    F          76.020920     C
TEMP. WATER OUT = 154.42871   F          67.934404     C
TEMP. R-113 IN = 90.088066    F          32.233066     C
TEMP. R-113 OUT = 135.68483   F          57.533798     C

R-113 SAT. TEMP. = 106.77479  F          41.541552     C

MEAN WATER TEMP = 161.71544   F          71.977662     C


TOTAL WATER FLOW RATE  =      240.39114  LBM/HR
                              109.02092  KG/HR

WATER FLOW REMAINING LIQUID = 239.61464  LBM/HR
                              108.66877  KG/HR

WATER FLOW LEAVING AS STEAM = .77650025  LBM/HR
                              .35215431  KG/HR


R-113 FLOW RATE = 37.499066   LBM/HR     17.006379     KG/HR


TANK PRESSURE =               14.57331   PSIA
                              100468.399 PA

PARTIAL PRESSURE STEAM =      2.5844815  PSI
                              17817.415

PARTIAL PRESSURE R-113  =     11.988829  PSI
                              82650.986  PA
```

HEAT LOSS FROM WATER REMAINING LIQUID =			3492.0116 1023.1502	BTU/HR WATTS
HEAT GAIN FROM WATER TURNING TO STEAM =			763.42923 223.68275	BTU/HR WATTS
NET HEAT TRANSFERRED FROM WATER =			2728.5823 799.46743	BTU/HR WATTS
HEAT ADDED TO LIQUID R-113 =			136.41060 39.967946	BTU/HR WATTS
HEAT ADDED TO BOIL R-113 =			2398.1849 702.66185	BTU/HR WATTS
NET HEAD ADDED TO R-113 =			2707.1197 793.17894	BTU/HR WATTS
LMTD =	47.139740	F	26,188744	C
UA =	57.427548	BTU/LBM F	30.287289	WATTS/C
PINCH-POINT =	48.221376	F	26.789654	C

APPENDIX IV

DATA

This appendix contains, in tabular form, the data used to generate the curves presented in this paper. The data obtained from the experimental apparatus is provided in reduced form with the necessary results for each curve included. A list of variables used in these tables is included at the end of this section.

Table 1. Data for Figure 8

$\dot{m}_w$ (kg/hr)	$\dot{m}_R$ (kg/hr)	T_{wi} (°C)	T_{wo} (°C)	T_{Ri} (°C)	T_{Ro} (°C)	$P_v \times 10^4$ (P_a)	$P_a \times 10^4$ (P_a)	$Q_w/m_R \times 10^5$ (J/kg)	$Q_R/m_R \times 10^5$ (J/kg)
109	17.0	64.7	57.1	32.5	51.3	9.88	8.61	1.67	1.64
98	17.1	64.5	56.7	32.3	50.7	9.88	8.61	1.55	1.63
86	16.8	64.8	55.6	32.9	50.4	10.47	8.49	1.67	1.62
74	16.8	64.8	54.5	33.9	59.8	10.01	8.49	1.59	1.61
63	16.7	65.0	53.0	33.4	48.5	9.88	8.49	1.59	1.61
62	17.1	64.3	52.4	31.8	45.5	9.91	8.56	1.54	1.60
54	17.1	64.3	51.0	31.0	43.5	9.66	8.56	1.52	1.60
46	17.3	64.7	49.2	30.5	42.7	9.40	8.56	1.49	1.60
38	17.1	65.0	57.8	30.3	42.8	9.32		1.38	1.60

Table 2. Data for Figure 9

$\dot{m}_w$ (kg/hr)	$\dot{m}_R$ (kg/hr)	T_{wi} (°C)	T_{wo} (°C)	T_{Ri} (°C)	T_{Ro} (°C)	$P_v \times 10^4$ (P_a)	$P_a \times 10^4$ (P_a)	$Q_w/\dot{m}_R \times 10^5$ (J/kg)	$Q_R/\dot{m}_R \times 10^5$ (J/kg)
109	16.8	69.3	61.7	33.8	53.2	9.92	8.65	1.67	1.64
98	17.0	69.3	61.1	32.9	53.3	9.84	8.65	1.58	1.65
86	16.8	69.3	60.1	32.6	52.8	9.88	8.65	1.58	1.65
80	16.9	69.4	59.1	31.5	52.3	9.93	8.66	1.69	1.65
74	16.9	69.3	58.8	32.4	52.2	9.92	8.65	1.58	1.64
69	17.0	69.4	57.8	31.6	51.4	9.68	8.66	1.62	1.65
63	16.9	69.3	57.1	32.2	51.1	9.92	8.65	1.56	1.64
62	17.3	68.9	55.6	30.6	49.6	10.24	8.59	1.69	1.64
58	16.7	68.9	55.4	32.3	49.8	9.53	8.64	1.61	1.63
58	17.0	68.8	55.2	31.4	48.8	9.87	8.60	1.64	1.63
54	17.0	69.4	54.9	32.9	48.9	9.63	8.62	1.60	1.62
51	16.8	69.2	54.8	32.2	49.9	9.84	8.65	1.52	1.63
50	17.1	69.0	53.5	31.7	48.6	9.70	8.60	1.58	1.62
46	17.3	69.0	52.9	33.2	47.1	9.54	8.62	1.50	1.60
42	16.9	69.2	51.7	32.2	47.4	9.53	8.64	1.52	1.61
42	17.1	69.1	51.4	31.5	47.2	9.53	8.60	1.53	1.62
38	17.4	68.9	50.1	32.2	45.3	9.55	8.62	1.46	1.60
38	16.9	68.9	50.5	31.3	46.4	9.74	8.60	1.47	1.61
34	16.6	68.8	49.5	31.9	45.4	9.44	8.64	1.39	1.60
34	17.0	68.9	49.9	31.2	45.2	9.49	8.60	1.34	1.61
30	16.9	69.0	48.3	31.1	44.5	9.44	8.60	1.30	1.60
26	16.8	69.1	49.0	31.6	44.3	9.36	8.64	1.16	1.60
26	16.7	69.1	47.8	31.0	44.1	9.36	8.60	1.06	1.60

Table 3. Data for Figure 10

$\dot{m}_w$ (kg/hr)	$\dot{m}_R$ (kg/hr)	T_{wi} (°C)	T_{wo} (°C)	T_{Ri} (°C)	T_{Ro} (°C)	$P_v \times 10^4$ (P_a)	$P_a \times 10^4$ (P_a)	$Q_w/\dot{m}_R \times 10^5$ (J/kg)	$Q_R/\dot{m}_R \times 10^5$ (J/kg)
109	17.0	76.0	67.9	32.2	57.5	10.04	8.61	1.69	1.68
98	16.9	76.3	67.4	32.0	57.6	10.00	8.61	1.64	1.68
86	16.8	75.9	66.2	31.6	57.1	9.96	8.61	1.61	1.68
74	16.9	76.4	64.8	31.7	56.3	9.96	8.61	1.69	1.68
63	16.8	76.0	62.8	31.7	54.9	9.96	8.61	1.65	1.67
62	16.8	75.6	63.1	30.3	51.3	9.65	8.56	1.57	1.66
54	16.9	75.9	61.0	30.5	50.8	9.65	8.56	1.64	1.65
46	16.9	75.8	58.8	30.4	50.1	9.74	8.56	1.61	1.65
38	17.1	75.9	56.2	30.4	47.3	9.57	8.56	1.56	1.63
30	16.9	75.5	52.1	30.3	44.8	9.65	8.56	1.51	1.61
22	17.2	76.0	48.6	30.2	42.6	9.22	8.56	1.25	1.60

Table 4. Data for Figure 12

$\dot{m}_w$ (kg/hr)	$\dot{m}_R$ (kg/hr)	T_{wi} (°C)	T_{wo} (°C)	T_{Ri} (°C)	T_{Ro} (°C)	$P_v \times 10^4$ (P_a)	$P_a \times 10^4$ (P_a)	$\Delta T'$ (°C)	UA (watts/°C)
109	17.0	64.7	57.1	32.5	51.3	9.88	8.61	22.2	41.9
109	16.8	69.3	61.7	33.8	53.2	9.92	8.65	27.2	35.5
109	17.0	76.0	67.9	32.2	57.5	10.05	8.61	34.6	30.3
109	16.8	81.8	73.3	32.8	62.0	9.92	8.49	42.4	27.4
54	13.6	66.0	54.1	28.5	49.0	9.04	8.62	25.9	29.8
54	13.8	68.6	56.9	27.2	50.9	9.14	8.60	28.7	27.7
54	13.5	72.3	59.6	28.8	52.3	9.22	8.63	32.3	25.2

Table 5. Data for Figure 13

$\dot{m}_w$ (kg/hr)	$\dot{m}_R$ (kg/hr)	T_{wi} (°C)	T_{wo} (°C)	T_{Ri} (°C)	T_{Ro} (°C)	$P_v \times 10^4$ (P_a)	$P_a \times 10^4$ (P_a)	$\Delta T'$ (°C)	UA (watts/°C)
109	16.8	69.3	61.7	33.8	53.2	9.92	8.65	27.2	35.5
98	17.0	69.3	61.1	32.9	53.3	9.84	8.65	27.5	36.0
86	16.8	69.3	60.1	32.6	52.8	9.88	8.65	27.2	35.5
80	16.9	69.4	59.1	31.5	52.3	9.93	8.66	27.0	35.3
74	16.9	69.3	58.8	32.4	52.2	9.92	8.65	26.7	35.7
69	17.0	69.4	57.8	31.6	51.4	9.68	8.66	27.7	35.4
63	16.9	69.3	57.1	32.2	51.1	9.92	8.65	26.7	35.9
109	17.0	76.0	67.9	32.2	57.5	10.05	8.61	34.6	30.3
98	16.9	76.3	67.4	31.9	57.6	10.00	8.61	34.9	30.3
86	16.8	75.9	66.2	31.6	57.1	9.96	8.61	34.6	30.3
74	16.9	76.4	64.8	31.7	56.3	9.96	8.61	34.9	30.2
63	16.8	76.0	62.8	31.7	54.9	9.96	8.61	34.1	30.1
109	17.0	64.7	57.1	32.5	51.3	9.88	8.61	22.2	41.9
98	17.1	64.5	56.7	32.3	50.7	9.88	8.61	22.0	41.6
86	16.8	64.8	55.6	32.9	50.4	10.48	8.49	20.3	41.2
74	16.8	64.8	54.5	33.9	49.8	10.00	8.49	21.7	42.5
109	16.8	81.8	73.3	32.8	62.0	9.92	8.49	42.3	27.4
98	16.8	81.9	72.8	32.6	62.0	10.05	8.49	41.9	27.6
86	16.8	82.1	71.7	32.7	61.2	10.01	8.49	41.9	27.3
74	16.9	82.2	70.4	32.6	60.1	10.01	8.49	41.7	27.2
63	16.9	81.7	68.3	32.4	58.7	9.97	8.49	40.8	27.4

Table 6. Data for Figure 14

$\dot{m}_w$ (kg/hr)	$\dot{m}_R$ (kg/hr)	T_{wi} (°C)	T_{wo} (°C)	T_{Ri} (°C)	T_{Ro} (°C)	$P_v \times 10^4$ (P_a)	$P_a \times 10^4$ (P_a)	$\Delta T'$ (°C)	UA (watts/ °C)
58	16.3	68.8	54.0	32.7	49.0	10.25	8.64	24.7	35.5
58	15.5	68.7	56.1	32.4	50.2	9.45	8.64	27.5	33.4
58	15.3	68.9	54.7	32.4	48.9	9.74	8.64	26.4	32.5
58	14.2	68.9	56.7	28.2	50.5	9.28	8.64	28.4	28.4
58	13.1	68.8	57.2	28.1	50.2	9.15	8.64	28.7	25.8

Table 7. Data for Figure 15

$\dot{m}_w$ (kg/hr)	$\dot{m}_R$ (kg/hr)	T_{wi} (°C)	T_{wo} (°C)	T_{Ri} (°C)	T_{Ro} (°C)	$P_v \times 10^4$ (P_a)	$P_a \times 10^4$ (P_a)	$\Delta T'$ (°C)	ΔT_s (°C)
109	16.8	69.3	61.7	33.8	53.2	9.92	8.65	27.2	11.1
98	17.0	69.3	61.1	32.9	53.3	9.84	8.65	27.5	11.4
86	16.8	69.3	60.1	32.6	52.8	9.88	8.65	27.2	10.7
80	16.9	69.4	59.1	31.5	52.3	9.93	8.66	27.0	9.9
74	16.9	69.3	58.8	32.4	52.2	9.92	8.65	26.9	9.7
69	17.0	69.4	57.8	31.6	51.4	9.68	8.66	27.7	9.7
63	16.9	69.3	57.1	32.2	51.1	9.92	8.65	26.7	8.5
62	17.3	65.9	55.6	30.6	49.6	10.24	8.59	24.9	5.6
58	16.7	68.9	55.4	32.3	49.8	9.53	8.64	27.3	8.2
58	17.0	68.8	55.2	31.4	48.8	9.87	8.60	25.9	5.8
54	17.0	69.4	54.9	32.9	48.9	9.63	8.62	27.3	6.8
51	16.8	69.2	54.5	32.2	49.9	9.84	8.65	26.6	7.3
50	17.1	69.0	53.5	31.7	48.6	9.70	8.60	26.6	6.2
46	17.3	69.0	52.9	33.2	47.1	9.54	8.62	26.8	4.9
42	16.9	69.2	51.7	32.2	47.4	9.53	8.64	27.1	5.3
42	17.1	69.1	51.4	31.5	47.2	9.53	8.60	27.0	5.1
38	17.4	68.9	50.1	32.2	45.3	9.55	8.62	26.4	2.7
38	16.9	68.9	50.5	31.3	46.4	9.74	8.60	26.0	3.4
34	16.6	68.8	49.5	31.9	45.4	9.44	8.64	26.7	3.2
34	17.0	68.9	49.9	31.2	45.2	9.49	8.60	26.6	2.9
30	16.9	69.0	48.3	31.1	44.5	9.44	8.60	26.8	2.2
26	16.8	69.1	49.0	31.6	44.3	9.36	8.64	27.1	2.3
26	16.7	69.1	47.8	31.0	44.1	9.36	8.60	27.1	2.0
109	17.0	64.7	57.1	32.5	51.3	9.88	8.61	22.2	8.9

Table 7 (continued)

98	17.1	64.5	56.7	32.3	50.7	9.88	8.61	22.0	8.1
86	16.8	64.8	55.6	32.9	50.4	10.48	8.49	20.3	5.8
74	16.8	64.8	54.5	33.9	49.8	10.00	8.49	21.7	6.6
63	16.7	65.0	53.0	33.4	48.5	9.88	8.56	22.0	5.5
62	17.1	64.3	52.4	31.8	45.5	9.91	8.56	20.6	1.8
54	17.1	64.3	51.0	31.0	43.5	9.66	8.56	21.2	0.4
46	17.3	64.7	49.2	30.5	42.7	9.40	8.56	22.3	0.2
38	17.1	65.0	47.8	30.3	42.8	9.32	8.61	22.9	0.6
109	17.0	76.0	67.9	32.2	57.5	10.05	8.61	34.6	16.1
98	16.9	76.3	67.4	31.9	57.6	10.00	8.61	34.9	16.3
86	16.8	75.9	66.2	31.6	57.1	9.96	8.61	34.6	15.7
74	16.9	76.4	64.8	31.7	56.3	9.96	8.61	34.9	14.8
63	16.8	76.0	62.8	31.7	54.9	9.96	8.61	34.1	13.0
62	16.8	75.6	63.1	30.3	51.3	9.65	8.56	34.0	9.6
54	16.9	75.9	61.0	30.5	50.8	9.65	8.59	34.1	9.0
46	16.9	75.8	58.8	30.4	50.1	9.74	8.56	33.6	7.9
38	17.1	75.9	56.2	30.4	47.3	9.57	8.56	33.7	5.0
30	16.9	75.5	52.1	30.3	44.8	9.65	8.56	32.6	1.8
22	17.2	76.0	48.6	30.2	42.6	9.22	8.56	34.4	1.0

Table 8. Data for Figure 17

$\dot{m}_w$ (kg/hr)	$\dot{m}_R$ (kg/hr)	T_{wi} (°C)	T_{wo} (°C)	T_{Ri} (°C)	T_{Ro} (°C)	$P_v \times 10^4$ (P_a)	$P_a \times 10^4$ (P_a)	$\Delta T'$ (°C)	ΔT_p (°C)
109	16.8	69.3	61.7	33.8	53.2	9.92	8.65	27.2	19.8
98	17.0	69.3	61.1	32.9	53.3	9.84	8.65	27.5	19.6
86	16.8	69.3	60.1	32.6	52.8	9.88	8.65	27.2	18.4
80	16.9	69.4	59.1	31.5	52.3	9.93	8.66	27.0	17.2
74	16.9	69.3	58.8	32.4	52.2	9.92	8.65	26.9	16.9
69	17.0	69.4	57.8	31.6	51.4	9.68	8.66	27.7	16.6
63	16.9	69.3	57.1	32.2	51.1	9.92	8.65	26.7	15.1
62	17.3	68.9	55.6	30.6	49.6	10.24	8.59	24.9	12.4
58	16.7	68.9	55.4	32.3	49.8	9.53	8.64	27.3	14.4
58	17.0	68.8	55.2	31.4	48.8	9.87	8.60	25.9	13.0
54	17.0	69.4	54.9	32.9	48.9	9.63	8.62	27.3	13.5
51	16.8	69.2	54.8	32.2	49.9	9.84	8.65	26.6	13.0
50	17.1	69.0	53.5	31.7	48.6	9.70	8.60	26.6	11.9
46	17.3	69.0	52.9	33.2	47.1	9.54	8.62	26.8	11.5
42	16.9	69.2	51.7	32.2	47.4	9.53	8.64	27.1	10.5
42	17.1	69.1	51.4	31.5	47.2	9.53	8.60	27.0	10.2
38	17.4	68.9	50.1	32.2	45.3	9.55	8.62	26.4	8.6
38	16.9	68.9	50.5	31.3	46.4	9.74	8.60	26.0	8.6
34	16.6	68.8	49.5	31.9	45.4	9.44	8.64	26.7	8.4
34	17.0	68.9	49.9	31.2	45.2	9.49	8.60	26.6	8.8
30	16.9	69.0	48.3	31.9	44.5	9.44	8.60	26.8	7.4
26	16.8	69.1	49.0	31.6	44.3	9.36	8.64	27.1	8.4
26	16.7	69.1	47.8	31.0	44.1	9.36	8.60	27.1	7.2

Table 8. (continued)

109	17.0	64.7	57.1	32.5	51.3	9.88	8.61	22.2	15.0
98	17.1	64.5	56.7	32.3	50.7	9.88	8.61	22.0	14.5
86	16.8	64.8	55.6	32.9	50.4	10.48	8.49	20.3	11.5
74	16.8	64.8	54.5	33.9	49.8	10.00	8.49	21.7	11.8
63	16.7	65.0	53.0	33.4	48.5	9.88	8.49	22.0	10.6
62	17.1	64.3	52.4	31.8	45.5	9.91	8.56	20.6	9.5
54	17.1	64.3	51.0	31.0	43.5	9.66	8.56	21.2	8.7
46	17.3	64.7	49.2	30.0	42.7	9.40	8.56	22.3	7.7
38	17.1	65.0	47.8	30.3	42.8	9.32	8.56	22.9	6.9
109	17.0	76.0	67.9	32.2	57.5	10.05	8.61	34.6	26.8
98	16.9	76.3	67.4	31.9	57.6	10.00	8.61	34.9	26.5
86	16.8	75.9	66.2	31.6	57.1	9.96	8.61	34.6	25.3
74	16.9	76.4	64.8	31.7	56.3	9.96	8.61	34.9	23.8
63	16.8	76.0	62.8	31.7	54.9	9.96	8.61	34.1	21.5
62	16.8	75.6	63.1	30.3	51.3	9.65	8.56	34.0	22.9
54	16.9	75.9	61.0	30.5	50.8	9.65	8.59	34.1	20.0
46	16.9	75.8	58.8	30.4	50.1	9.74	8.56	33.6	17.5
38	17.1	75.9	56.2	30.4	47.3	9.57	8.56	33.7	15.1
30	16.9	75.5	52.1	30.3	44.8	9.65	8.56	32.6	10.7
22	17.2	76.0	48.6	30.2	42.6	9.22	8.56	34.4	9.0

Table 9. Data for Figure 18

$\dot{m}_w$ (kg/hr)	$\dot{m}_R$ (kg/hr)	T_{wi} (°C)	T_{wo} (°C)	T_{Ri} (°C)	T_{Ro} (°C)	$P_v \times 10^4$ (P_a)	$P_a \times 10^4$ (P_a)	$\Delta T'$ (°C)	St	G
109	17.0	64.7	57.1	32.5	51.3	9.88	8.61	22.2	9.63	5.00
98	17.1	64.5	56.7	32.3	50.7	9.88	8.61	22.0	9.51	5.04
86	16.8	64.8	55.6	32.9	50.4	10.47	8.49	20.3	9.59	5.45
74	16.8	64.8	54.5	33.9	49.8	10.01	8.49	21.7	9.89	5.15
109	16.8	69.3	61.7	33.8	53.2	9.29	8.65	27.2	8.26	4.36
98	17.0	69.3	61.1	32.9	53.3	9.84	8.65	27.5	8.27	4.28
86	16.8	69.3	60.1	32.6	52.8	9.88	8.65	27.2	8.31	4.31
80	16.9	69.4	59.1	31.5	52.3	9.93	8.66	27.0	8.17	4.31
74	16.9	69.3	58.8	32.4	52.2	9.92	8.65	26.9	8.26	4.33
69	17.0	69.4	57.8	31.6	51.4	9.68	8.66	27.7	8.14	4.25
63	16.9	69.3	57.1	32.2	51.1	9.92	8.65	26.7	8.30	4.37
62	17.3	68.9	55.6	30.6	49.6	10.24	8.59	24.9	8.07	4.70
58	16.7	68.9	55.4	32.3	49.8	9.53	8.64	27.3	8.39	4.34
58	17.0	68.8	55.2	31.4	48.8	9.87	8.60	25.9	8.06	4.52
109	17.0	76.0	67.9	32.2	57.5	10.05	8.61	34.6	6.97	3.69
98	16.9	76.3	67.4	31.9	57.6	10.00	8.61	34.9	7.00	3.63
86	16.8	75.9	66.2	31.6	57.1	9.96	8.61	34.6	7.05	3.63
74	16.9	76.4	64.8	31.7	56.3	9.96	8.61	34.9	6.97	3.60
63	16.8	76.0	62.8	31.7	54.9	9.96	8.61	34.1	7.00	3.64
62	16.8	75.6	63.1	30.3	51.3	9.65	8.56	34.0	6.34	3.62
54	16.9	75.9	61.0	30.5	50.8	9.65	8.56	34.1	6.45	3.64
46	16.9	75.8	58.8	30.4	50.1	9.74	8.56	33.1	6.61	3.69
58	16.3	68.8	54.0	32.7	49.0	10.25	8.64	24.7	8.54	4.84

Table 9. (continued)

58	15.5	68.7	56.1	32.4	50.2	9.45	8.64	27.5	8.43	4.29
58	15.3	68.9	54.7	32.4	48.9	9.74	8.64	26.4	8.31	4.55
58	14.2	68.9	56.7	28.2	50.5	9.28	8.64	28.4	7.83	4.21
58	13.1	68.8	57.2	28.1	50.2	9.15	8.64	28.7	7.72	4.19
109	16.8	81.8	73.3	32.8	62.0	9.92	8.49	42.3	6.37	3.21
98	16.8	81.9	72.8	32.6	62.0	10.05	8.49	41.9	6.41	3.20
86	16.8	82.1	71.7	32.7	61.2	10.01	8.49	41.9	6.35	3.18
74	16.9	82.2	70.4	32.6	60.1	10.01	8.49	41.7	6.30	3.16
63	16.9	81.7	68.3	32.4	58.7	9.97	8.49	40.8	6.27	3.18

G - $H^{(0.625)}(\dot{m}_w/\dot{m}_R)^{(0.142)}$

$\dot{m}_R$ - R-113 flow rate

$\dot{m}_w$ - Water flow rate

P_a - Atmospheric pressure

P_v - Vessel pressure

Q_w - Net heat lost from water

St - Stanton number

T_{Ri} - R-113 inlet temperature

T_{Ro} - R-113 outlet temperature

T_{wi} - Water inlet temperature

T_{wo} - Water outlet temperature

$\Delta T'$ - The difference between the water inlet temperature and the R-113 saturation temperature

ΔT_p - Pinch-point ΔT

ΔT_s - The difference between the R-113 outlet temperature and the R-113 saturation temperature

UA - UA factor

APPENDIX V

DISCUSSION OF ERROR

This discussion will be concerned with the assessment of the accuracy of the various quantities reported in this thesis. The accuracy of the data obtained from the experimental apparatus as determined by calibration is shown below:

Temperatures . . . . . $\pm$ 0.1 °C

Water flow rate. . . . . $\pm$ 1.5 liters/hr

R-113 flow rate. . . . . $\pm$ 0.2 liters/hr

To determine how these possible variations would extend to the accuracy of the calculated quantities used in this paper (i.e., Q_w, Q_R, UA, and ΔT_p), the following data, corresponding to a typical test, is used:

T_{wi} = 76.0 °C

T_{wo} = 67.9 °C

T_{Ri} = 32.2 °C

T_{Ro} = 57.5 °C

$\dot{m}_w$ = 109 kg/hr

$\dot{m}_R$ = 17 kg/hr

These values were changed by their possible variations in such a manner as to produce the maximum error in the calculated quantities. The results were recalculated using these new

temperatures and flow rates. The results of this procedure are shown below:

	Absolute Error	Relative Error
Q_w	37 watts	5%
Q_R	14 watts	2%
UA	0.5 watts/°C	2%
ΔT_p	0.2	1%
St	0.3	5%

These variations represent the maximum possible error for the example data point. Since this is a typical data point, these values of error also represent a reasonable approximation for estimating the accuracy of the remaining data points reported in this paper.